

**VOLUMETRIC ESTIMATION OF AGBEJU FIELD, NIGER DELTA
NIGERIA, USING 3D SEISMIC AND WELL LOG DATA**

BY

Biebele Joy DIRI

PSC1503491

**DEPARTMENT OF GEOLOGY
FACULTY OF PHYSICAL SCIENCES
UNIVERSITY OF BENIN
BENIN CITY**

SEPTEMBER, 2023

**VOLUMETRIC ESTIMATION OF AGBEJU FIELD, NIGER DELTA
NIGERIA, USING 3D SEISMIC AND WELL LOG DATA**

BY

Biebele Joy DIRI

PSC1503491

**A PROJECT WORK SUBMITTED TO THE DEPARTMENT OF
GEOLOGY, FACULTY OF PHYSICAL SCIENCES, UNIVERSITY OF
BENEIN, IN PARTIAL FULFILMENT OF THE REQUIREMENT FOR
THE AWARD OF A BACHELOR OF SCIENCE DEGREE (B.Sc)
GEOLOGY**

SEPTEMBER, 2023

CERTIFICATION

This is to certify that Biebele Joy DIRI, MAT. NO. PSC1503491 carried out this project in fulfilment for the award of Bachelor of Science (B.Sc.) Degree in Geology.

DR S.A. SALAMI
(HEAD OF DEPARTMENT)

DATE

DR. A. OGBAMIKHUMI
(SUPERVISOR)

DATE

DEDICATION

I hereby dedicate this work to Almighty God for his provisions of life, unmerited favour and wisdom to complete this undergraduate research project. Also to my parents, Mr and Mrs Alfred Diri who have provided support and have been keen for my success in life.

ACKNOWLEDGEMENT

My utmost gratitude goes to my Almighty God for seeing me through my stay in the University of Benin.

I am deeply and truly indebted to my project supervisor, Dr A. Ogbamikhumi for his kind supervision, support and motivation which went beyond academic bounds.

I heartily appreciate my Parents, Mr and Mrs Alfred Diri, my guardian Mr Christopher Odeh and other members of my family. I say God bless you for the prayers and support you gave me throughout the program.

I am also grateful to my academic adviser, Dr Mrs T. Andre-Obayanju for all the advice, support and encouragement she showed me throughout my stay in the department.

I also acknowledge the effort and dedication of all members of staff in the Department of Geology for providing the necessary education and support throughout my stay.

Finally, to all my supporters and well-wishers, May the Good Lord Jesus reward you abundantly.

TABLE OF CONTENTS

CERTIFICATION	ii
DEDICATION	iii
ACKNOWLEDGEMENT	iv
LIST OF FIGURES	ix
LIST OF TABLES	xi
LIST OF EQUATIONS	xii
ABSTRACT	xiii
CHAPTER ONE	1
INTRODUCTION	1
1.1 GENERAL INTRODUCTION	1
1.2 BACKGROUND THEORY	2
1.2.1 SEISMIC EXPLORATION	2
1.2.2 PETROPHYSICAL EVALUATION	5
1.4 OBJECTIVES	7
1.5 SCOPE OF STUDY	8
1.6 LOCATION OF STUDY FIELD	9

CHAPTER TWO	10
LITERATURE REVIEW	10
2.1 REVIEW OF RELATED PREVIOUS WORK	10
2.2 GEOLOGICAL SETTING OF THE STUDY AREA	12
2.2.1 GEOLOGIC FRAMEWORK OF THE NIGER DELTA BASIN	12
2.2.2 TECTONIC AND STRUCTURAL SETTTING OF THE NIGER DELTA BASIN .	12
2.2.3 SEDIMENTARY FILL OF THE NIGER DELTA BASIN	16
2.2.4 STRATIGRAPHY OF THE NIGER DELTA	17
2.2.5 HYDROCARBON OCCURRENCE	19
CHAPTER THREE	24
MATERIALS AND METHODOLOGY	24
3.1 MATERIALS	24
3.2 AVAILABLE DATA	24
3.3 WORKFLOW	24
3.4 DATA LOADING AND QUALITY CHECK	24
3.4.1 SEISMIC DATA	25
3.4.2 WELL LOG DATA	26

3.5 DATA INTERPRETATION	27
3.5.1 WELL LOG CORRELATION	27
3.5.2 PETROPHYSICAL EVALUATION	27
3.5.3 WELL TO SEISMIC TIE	30
3.5.4 FAULT MAPPING	31
3.5.5 HORIZON MAPPING	31
3.5.6 TIME STRUCTURAL MAP	31
3.5.7 DEPTH STRUCTURAL MAP	31
3.5.8 SEISMIC ATTRIBUTE ANALYSIS	32
3.5.9 HYDROCARBON PROSPECT IDENTIFICATION	32
3.5.10 VOLUMETRIC ESTIMATION	32
CHAPTER FOUR	33
RESULTS AND DISCUSSION	33
4.1 RESULT AND DISCUSSION OF PETROPHYSICAL EVALUATION	33
4.1.1 WELL LOG CORRELATION	33
4.1.2 PETROPHYSICAL EVALUATION	34
4.2 RESULTS AND DISCUSSIONS OF 3D SEISMIC INTERPRETATION	38

4.2.1 FAULT INTERPRETATION	38
4.2.2 WELL TO SEISMIC TIE	40
4.2.3 HORIZON INTERPRETATION	41
4.2.4 TIME STRUCTURAL MAP	44
4.2.5 DEPTH STRUCTURAL MAP	44
4.2.6 SEISMIC ATTRIBUTE ANALYSIS AND PROSPECT IDENTIFICATION	47
4.3 VOLUMETRIC ESTIMATION	52
CHAPTER FIVE	53
CONCLUSION AND SUGGESTION FOR FURTHER WORK	53
5.1 CONCLUSION	53
5.2 SUGGESTION FOR FURTHER WORK	53
REFERENCES	53

LIST OF FIGURES

Figure 1: A basic log. A suite of logging measurements might include spontaneous potential, gamma ray, resistivity, neutron and density curves in a single presentation	8
Figure 2: Survey Map	9
Figure 3: Map of Niger Delta showing the study area (Whiteman, 1982).	13
Figure 4: Schematic diagram of a dip section from the Niger Delta showing the tectonic and structural elements. (Weber and Daukoru, 1975).	14
Figure 5: Niger Delta oil field structures and associated trap types. (Modified from Doust and Omatsola, 1990; Stacher, 1995).	15
Figure 6: The map view of the different Depobelts in the Niger Delta (Nwozor et al, 2013)	17
Figure 7: Stratigraphic column showing the three formations of the Niger Delta.	19
Figure 8: Workflow adapted	25
Figure 9: 3D view of study field when data was loaded.	26
Figure 10: Available well logs	27
Figure 11: well correlation of the sand bodies across the wells on the well section window.	33
Figure 12: Correlation and petrophysical evaluation of sand A across the wells	34
Figure 13: Correlation and petrophysical evaluation of sand B across the wells	35
Figure 14: Correlation and petrophysical evaluation of sand C across the wells	37
Figure 15: Faults shown on time slice of the variance edge seismic data	39
Figure 16: mapped faults along Xline on interpretation window.	40
Figure 17: Seismic to well tie using Agbeju 02 well.	41
Figure 18: Horizon mapping along Xline on interpretation window showing faults and the three horizons (A, B, C)	42
Figure 19: Horizons generated on map window with horizon A at top left, horizon B at top right and horizon C at bottom left.	43
Figure 20: Time structural maps for reservoir sand A at top left (a), reservoir sand B at top right (b) and reservoir sand C at bottom left (c).	45
Figure 21: Depth structural maps for reservoir sand A at top left (a), reservoir sand B at top right (b) and reservoir sand C at bottom left (c).	46
Figure 22: RMS amplitude seismic attribute for sand A top with identified prospects	47
Figure 23: Maximum amplitude seismic attribute for sand A top with identified prospects	48

Figure 24: RMS amplitude seismic attribute for sand B top with identified prospects	49
Figure 25 : Maximum amplitude seismic attribute for sand B top with identified prospects	50
Figure 26: RMS amplitude seismic attribute for sand C top with identified prospects	51
Figure 27: Maximum amplitude seismic attribute for sand C top with identified prospects	52

LIST OF TABLES

Table 1: Petrophysical evaluation of Sand A	35
Table 2: Petrophysical evaluation of Sand B	36
Table 3: Petrophysical evaluation of Sand C	38
Table 4: Volumetric estimation of each reservoir	52

LIST OF EQUATIONS

Equation 1: Gamma ray index (IGR).....	28
Equation 2: Shale volume (V_{sh}).....	28
Equation 3: Total porosity (Φ_{total}).....	28
Equation 4: Effective porosity (Φ_{eff}).....	29
Equation 5: Net to gross (NTG).....	29
Equation 6: Permeability (K).....	29
Equation 7: Irreducible water saturation (S_{Wirr}).....	30
Equation 8: Formation factor (F).....	30
Equation 9: Water saturation (SW).....	30
Equation 10: Gas initially in place (GIIP).....	32
Equation 11: Oil initially in place (OIP).....	32
Equation 12: Velocity modelling function (Z / TWT).....	44

ABSTRACT

This project work is focused on the volumetric estimation of Agbeju Field, Niger Delta using 3D seismic data and well logs. Data used for this project include 3-D seismic data in SEG-Y format and suites of five well logs (Agbeju 01, Agbeju 02, Agbeju 03, Agbeju 04 and Agbeju X01). 9 major faults and 24 minor faults were delineated on the seismic data. The lateral extent of 3 hydrocarbon bearing reservoirs were delineated and mapped as blocks (Sand A, Sand B and Sand C) and evaluated showing the petrophysical values across the reservoirs having average porosity of 0.32, average pay thickness of 98.46ft, average net-to-gross ratio of 0.84, and average water saturation of 0.625. From prospect identification, the area of the drilled prospects within the reservoirs ranges from 452.8634 acres – 1196.512 acres. The estimated volumes of hydrocarbons within the drilled prospects is given by Gas initially in place for Sand A (554MMSCF), Sand B (163MMSCF) and Sand C (258MMSCF) and Oil initially in place for Sand B (22.4MMBBL) and Sand C (83.93SMMBBL).

The result of the characterization of these reservoirs shows good productive sands with fair to good hydrocarbon saturation of 0.375, with sufficient hydrocarbon volumes necessary for field development and production.

CHAPTER ONE

INTRODUCTION

1.1 GENERAL INTRODUCTION

The offshore Niger-Delta region holds several giant oil and gas fields with a lot of exploration opportunities trapped in a variety of complex structural styles. Potential prospects extend through the continental shelf, the continental slope and into the deep-water environment within the offshore depobelt. The region has continued exploration, development and production activities and represents a major hydrocarbon province. (Anene et al., 2018).

A major challenge in the oil and gas industry involves the uncertainty in the volumetric estimation of hydrocarbon accumulations due to inadequate and poorly defined reservoir characterisation. The use of 3D seismic interpretation and well log evaluation can help provide better information on the reservoir properties and improved accuracy of economic viability and cost effectiveness during exploration stage through to the production stage. (El-Mowafy and Marfurt , 2008)

Integration of well log data for petrophysical evaluation of subsurface formations is a major aspect in formation evaluation in oil and gas industry. This is because well logs possess key information about the reservoir quality, reservoir extent and recoverable volume of hydrocarbon. (Asquith and Krygowski, 2004). Reservoir parameters such as porosity, shale volume, permeability, water saturation, net to gross, hydrocarbon saturation are derived by mathematical calculations using empirical formulas. These parameters will help determine the quality of the reservoir for exploitation. (Shepherd, 2009; Stacy et al., 2010; Okwoli et al., 2015; Obiora et al., 2016).

3D seismic interpretation helps to provide information on the nature of the various types of subsurface structures that can control the trapping of commercial quantities of hydrocarbon accumulations within a given surveyed area. Seismic attributes are useful for quantitative and qualitative analyses. Quantitative uses include prediction of reservoir properties such as porosity or lithology. Qualitative uses include identification of stratigraphic and structural features such as faults. (Leiphart and Hart, 2001; Sagan and Hart, 2006).

In Nigeria, the prolific hydrocarbon province is the Niger Delta basin. The Niger Delta is one of the largest hydrocarbon provinces in the world and is located in the Gulf of Guinea, on the

western coast of Africa and southern part of Nigeria, this clastic wedge continues to prograde seaward and contains the 12th largest recoverable hydrocarbons accumulation globally, with reserve estimates of over 34 billion barrels of oil and 93 trillion cubic feet of gas. Exploration is still on-going as new discoveries, mostly offshore, are made to further improve reserve estimates.

1.2 BACKGROUND THEORY

1.2.1 SEISMIC EXPLORATION

Seismic exploration involves the acquisition, processing and interpretation of seismic data for exploratory activities for the discovery of earth's resources such as hydrocarbons at great depths within the subsurface. It is an indirect geophysical exploration method whose property contrast is the varying response of earth materials to propagating acoustic waves. This method employs sending acoustic energy (sound waves) generated from the surface into the subsurface, as the sound waves propagate through the subsurface rocks. An interaction occurs whereby portions of the incident sound waves are transmitted while the remaining portions are reflected back to the surface. The surface where this interaction occurs is referred to as an "interface" in geophysical terminology; it marks the presence of a geological event which can subsurface rocks or even pore fluids. The reflectivity along this interface is produced as a result of the contrast in acoustic impedance (AI) between geological events. Acoustic impedance can also simply be the resistance of subsurface materials to the speed of propagating sound waves through it. AI is the product of the density of the subsurface rocks and the velocity of the sound waves propagating through it.

From this exploratory method, an acoustic image of the earth's subsurface can be produced as a reflectivity series. This reflectivity series comprises the acoustic response of the subsurface rocks and also the effect of filtering due to the earth's natural reflectivity series, this filtering effect is known as "convolution". For better interpretation, the filtering effect of the earth is reduced during data processing to give only the reflectivity series solely due to the subsurface rocks by a process known as "deconvolution".

a) SEISMIC DATA ACQUISITION

Seismic surveys are activities which employ the use of technical expertise, man power, planning and pieces of equipment for the acquisition of subsurface information as seismic data. We have

2D seismic survey which is used to acquire line data, 3D seismic surveys which is used to acquire volume data and 4D seismic surveys also referred to as time lapse 3D seismic surveys which is a repeated 3D seismic survey which introduces the time element after a period to further understand the area.

Seismic surveys are done on land (onshore) and on water bodies (offshore). The primary pieces of equipment used during seismic surveys are the seismic source of energy and the receivers. Onshore, seismic sources of energy include truck mounted vibratory devices and dynamite detonated in a shallow borehole. Offshore, we have pneumatic devices such as water guns and air guns which expels water or air into surrounding water to generate seismic energy, we also have sparkers, pingers and boomers that convert electrical energy into seismic energy. For receivers, we have geophones for land based surveys and hydrophones for offshore based surveys. These receivers are devices that convert the mechanical energy from vibrations on the surface into electrical energy that are transmitted via cables and recorded on a seismogram.

The acquisition geometry which is the configuration of the source elements and the receiver elements which can be arranged in circular, square or triangular loops in a straight line or zig-zag lines depends on the survey objectives, nature of subsurface geology, noise reduction, data resolution and logistics.

b) SEISMIC DATA PROCESSING

The purpose of seismic data processing is to reduce noise elements and improve the resolution of the reflectivity series due to geologic events within the data. Some steps are employed during processing which includes Demultiplexing, Deconvolution, Static correction, Dynamic correction, Stacking and Migration.

Demultiplexing: The data recorded on the seismogram during data acquisition is usually in time sequential form. For better processing and interpretation, demultiplexing transforms the data to trace sequential form.

Deconvolution: This is an inverse filtering technique used to remove the earth's filtering effect and thus enhance the reflectivity series that arises solely due to the subsurface geology. It attempts to reduce the resulting wavelet to resemble a spike which can be described as a result of the true subsurface geology.

Static correction: This is done to remove the effect of placing the source and receiver elements on uneven topography. It is also used to reconfigure the placement of the source and receiver elements to equal depth below the low velocity layer.

Dynamic correction: The configuration of the shot – receiver pairs is arranged such that it generates a common mid point (CMP) reflection points along a reflector. As a result of this configuration, there is difference in travel time of the reflected waves due to increasing offset distances. The Normal move out (NMO) is the difference between the zero offset and non zero offset travel times. To correct for NMO, we extract the seismic velocities across the seismic data, the depth to the target reflector. Using mathematical calculations, the time difference due to offset distances are removed and each shot – receiver pairs are at zero offset. This places all seismic traces at the CMP at similar elevation levels before stacking.

Stacking: This process involves the the summation of all seismic traces from various offsets distances associated with a common mid point after dynamic correction have been applied. It enhances the signal-noise ratio and hence signals due to the true geology are enhanced.

Migration: This is the process where the reflected signals are repositioned to their actual depth to show the geological event (reflector) at its true position. Multiples are signals that have been reflected on multiple interfaces within the subsurface before reaching the recorder on the surface.

c) SEISMIC INTERPRETATION

The first interpretation step to take is to ‘tie’ the seismic data to existing well log data to identify what the important reflector events corresponds to in the well data. These reflector events / horizons are then picked across the seismic data; faults are also picked in the same manner. The integration of these faults and horizons define the structuration of the field which is then mapped out and potential trapping mechanisms are identified.

Seismic inversion allows seismic data to not only be seen as reflectivity data with a characteristic seismic pulse but also in terms of acoustic impedance. It allows the removal of the effect of the seismic wavelet and represents the data as a function of rock layer property (acoustic impedance). It is a complex process with careful calibration to well data and broad knowledge of the subsurface geology.

When interpretation is complete, the interpreted surfaces which were generated in time domain must be converted to depth. This can be achieved by determining the time to depth relationship by velocity modelling using interval velocities or stacking velocities across the seismic volume. Seismic attributes are a post stack processing algorithm that allows seismic data to be investigated with advanced techniques. Structural attributes of the data such as dip, azimuth and degree of uniformity can help to understand structural styles or to interpret fault distribution within a basin. Attributes generated from the amplitude analysis of the data can show insights into rock properties, such as porosity and permeability, and in some cases pore fluid nature, such as hydrocarbon saturation.

1.2.2 PETROPHYSICAL EVALUATION

a) WELL LOGS

Well logs or wireline logs are continuous records of physical properties measured from subsurface rocks against the depth of investigation. It is used to generate subsurface information that is critical for the identifying and evaluating hydrocarbon bearing reservoirs and source rocks from wells during exploratory activities, further characterisation of a hydrocarbon field assisting in volumetric estimation, geological and geophysical modelling during appraisal and field development. It is also used to monitor and provide information on the amount of recoverable hydrocarbons left in a reservoir during its production lifetime.

Acquisition of well logs involves lowering a sonde into the well after the drill string has been retrieved or it can be acquired while drilling operations are ongoing. The sonde is a logging tool equipped with measurement sensors that are used in measuring physical properties of subsurface rocks such as natural gamma ray radioactivity, resistivity, formation bulk density etc. This measured information is transmitted electrically via cables to a recording and processing logging unit on the surface.

b) GAMMA RAY LOG

This is a continuous record of a formation's response to natural radioactivity along a given depth. The radiation is generated naturally from constituent uranium, thorium and potassium within the

formation. The simple gamma ray log gives the radioactivity of the combined three elements, while spectral gamma ray log show the contribution of the individual elements to the overall measured radioactivity.

Gamma ray logs are used to quantify shale volume. Qualitatively, it is used to identify lithologies, correlate different lithologies and to identify shale content within a formation.

c) RESISTIVITY LOG

This log is a continuous record of a formation's resistivity along a given depth, it is the resistance of the rock to the passage of an electric current. Most rock materials are essentially insulating, while their pore fluids (brine) are conductive. Hydrocarbons are less conductive, and on contrary, they are infinitely resistive. The quantitative use of resistivity log measurements is one main domain of petrophysical studies used is to detect and quantify hydrocarbons saturation. It is also used to identify the water saturation contained in the hydrocarbon bearing reservoir.

d) SONIC LOG

This is a continuous record of a formation's interval transit time along a given depth, it is the reciprocal of the velocity. It is an indication of the formation's ability to transmit sound waves. Qualitatively, it can be used for lithology identification. Quantitatively, the sonic log is used to evaluate porosity. In seismic interpretation, it can be used to give velocity profiles such as interval velocities, which can be calibrated with the seismic section. The acoustic impedance log is generated using the product of density and the velocity derived from the sonic log. It is the first step required for generating a synthetic seismic trace during well to seismic tie.

e) DENSITY LOG

This is a continuous record of a formation bulk density along a given depth. This is the total density of a rock including the rock matrix and the constituent pore fluids. The formation bulk density is a function of the density of the mineralogy of the rock (matrix) and the volume of pore fluids (pore spaces). Quantitatively, the density log is used to calculate porosity. Qualitatively, it can help as a lithology indicator.

f) NEUTRON LOG

This is a continuous record of a formation's reaction to fast neutron bombardment along a given depth. It is given in neutron porosity units, which is related to a formation's hydrogen index (HI), a measure of the hydrogen content. It is defined as the wt % hydrogen in the formation/wt % hydrogen in water, where HI of water equals 1. However, the interest in water is as a pore fluid and porosity indicator. Quantitatively, it is used for porosity calculations. Qualitatively, it helps discriminate between gas and oil. When combined with density log on compactible scales, it provides better lithology identification compared to other logs.

g) NEUTRON DENSITY COMBINATION LOG

This is a combination porosity log. It is used primarily as a porosity device, it is also used to identify and delineate different lithologies and also detect gas-bearing zones. The Neutron-Density combination log also shows the change in character of the neutron-density curves in response to oil- or water-bearing sands and gas-bearing sands. The gas effect occurs in a gas-bearing zone when neutron porosity values increases and bulk density values reduces.

1.3 AIM

The aim of this research is to characterise the hydrocarbon bearing reservoirs and estimate the volume of the hydrocarbons in place within Agbeju field.

1.4 OBJECTIVES

1. Identification and delineation of hydrocarbon bearing reservoir(s) and petrophysical evaluation of these reservoir(s) across the wells.
2. Correlation of well logs.
3. 3D seismic interpretation; faults and horizons mapping to understand the structural framework and trapping mechanisms of the study field.
4. Volumetric estimation of all identified hydrocarbon bearing reservoir(s).

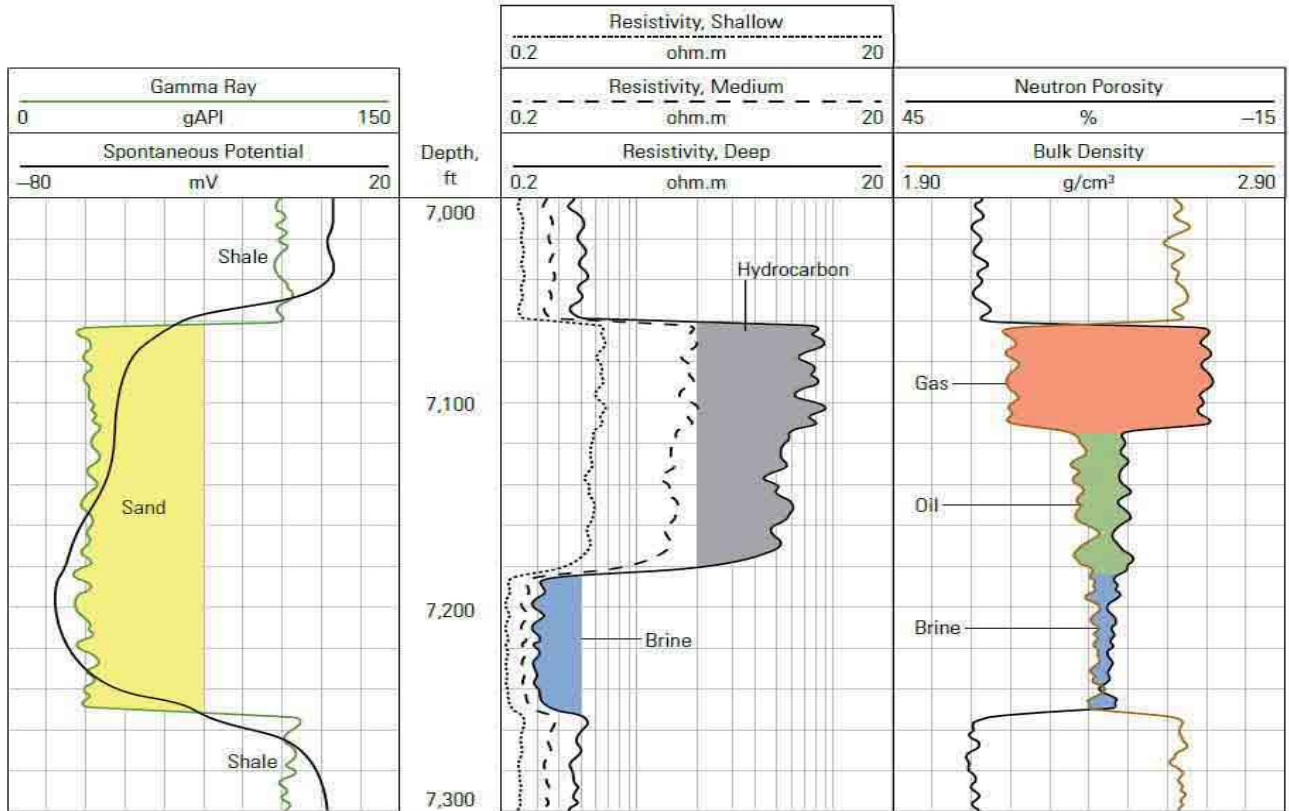


Figure 1: A basic log. A suite of logging measurements might include spontaneous potential, gamma ray, resistivity, neutron and density curves in a single presentation. (Varhaug, 2016).

1.5 SCOPE OF STUDY

Petrophysical evaluation: Well log data was loaded where correlation of wells and petrophysical study of hydrocarbon bearing reservoirs was carried out using the Schlumberger Petrel software.

Seismic interpretation: Interpretation of the 3-D seismic data of the study field using Schlumberger Petrel software to determine the structural framework of the study field. Well to seismic tie was done to identify the location of the well within the seismic data.

Generation of the time structural map: structural maps would be produced for the mapped horizon(s) to understand the geometry and configuration of the structures within the study field.

Generation of the depth structural map: Depth structural maps would be produced from the time structural maps using a time to depth relationship derived from seismic to well tie.

Prospect identification: Using seismic attributes to generate direct hydrocarbon indicator (DHI), we can highlight prospect areas. Also, using well location, we can measure the extent of the prospect area.

Volumetric estimation: Using the derived data from the petrophysical evaluation and 3D seismic interpretation, key parameters are used to estimate the volume of hydrocarbon in place within the field.

1.6 LOCATION OF STUDY FIELD

Agbeju field is a fictitious name given to an area within the offshore depobelt of the Niger Delta. The location of the field is given between latitudes $4^{\circ}00'47.8981''\text{N}$ and $4^{\circ}09'11.8906''\text{N}$ and longitudes $7^{\circ}28'01.6715''\text{E}$ and $7^{\circ}36'24.2826''\text{E}$. The Niger Delta region of Nigeria is approximately 85km towards the Atlantic Ocean lying between latitude $5^{\circ}00'$ and $5^{\circ}25'\text{N}$ and longitudes $7^{\circ}35'$ and $8^{\circ}00'\text{E}$.

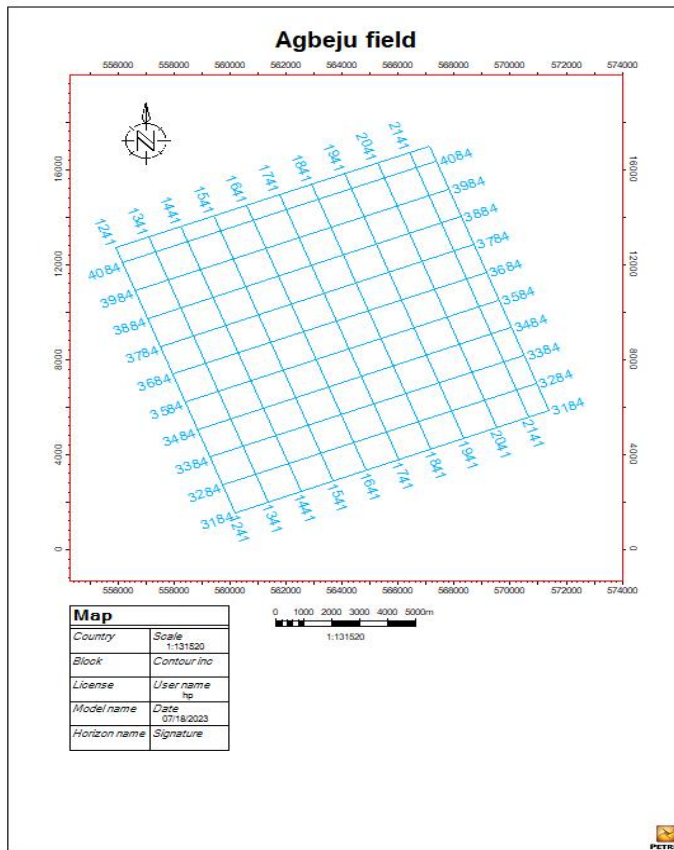


Figure 2: Survey Map of Agbeju field.

CHAPTER TWO

LITERATURE REVIEW

2.1 REVIEW OF RELATED PREVIOUS WORK

(Osinowo et al., 2018) in their work “Reservoir description and characterization of Eni field Offshore Niger Delta, southern Nigeria” characterised and described Eni Field, offshore Niger Delta. This field, which has been experiencing production decline with increased water output, has been studied using a combination of stratigraphic analyses, structural mapping of 3D seismic data, reservoir property modelling and petrophysical evaluation of sixty (60) wireline logs, and production data. The constructed reservoir structural framework and spatial distribution of the reservoir properties have aided in determination of the optimal placement of proposed wells in providing the necessary information of the best production plan to efficiently drain the defined hydrocarbon bearing reservoirs.

(Okpogo et al., 2018) in their work “Reservoir characterization and volumetric estimation of Orok Field Niger Delta Province using well logs, 3-D seismic and check-shot data” characterised the field and described four gas-bearing reservoirs having effective porosity ranging between 18% and 20% and hydrocarbon saturation between 77% and 90%. Hydrocarbon volumetric estimation for the two viable prospects showed 151 bbl/ft³ and 286 bbl/ft³ of gas respectively.

(Illo et al., 2022) in their work “Prospect identification and reservoir characterization using seismic and petrophysical data in ‘Famito’ field, onshore Niger Delta, Nigeria” studied an integration of seismic and well logs data from six wells has been carried out across Famito field. Well log interpretation and correlation delineated hydrocarbon-bearing reservoirs (F-1000, G-1000, and H-1000). Structural analyses has been carried out using seismic data, which was used to highlight major, antithetic, and synthetic faults with three horizons that were mapped and used to generate time structural maps. Petrophysical evaluation showed that reservoir F-1000 has very good porosity (22%–28%), volume of shale (25%–33%), and high hydrocarbon saturation (47%–90%) with an oil and gas phase. Similarly, G-1000 and H-1000 consists of shaly sands with very good average porosities (25% and 24%, respectively) and high average hydrocarbon saturations (66% and 71%, respectively).

(Omoja & Obiekezie, 2021) in their work “Evaluation of the petrophysical parameters in Uzot-field was carried out using Well log data” studied the D3100 reservoir found in wells Uz 004, Uz 005, U008 and Uz 011 with depth ranging from 5540ft - 5800ft across the four wells. The results of petrophysical evaluation showed the delineated reservoirs having porosity ranging from 21.40% - 33.80% indicating a suitable reservoir quality; permeability values ranging from 1314md - 18089md and hydrocarbon saturation ranging from 12.00% - 85.79% indicating high hydrocarbon content. These petrophysical properties shows that the D3100 reservoir can be considered satisfactory for hydrocarbon production.

(Wobo and Ideozu, 2022) in their work “Petrophysical evaluation and reservoir modelling of Kala Field, Eastern Niger Delta using 3-D Seismic in Seg-Y and suites of well logs”, characterised and showed normal faults trending NW-SE which were delineated. The reservoirs E and F were delineated in blocks (A, B and C) and modelled. The results of the petrophysical evaluation showed the reservoirs in blocks A, B and C in Reservoirs E and F having porosity (25% (A), 25% (B), and C 23%), permeability (291md (A), 300md (B), 1990md (C)), Net-to-Gross ratio (0.74, (A) 0.80 (B), 0.66 (C)), water saturation (45%, 39%,37%) and Stock tank oil initially in place (54.71mmstb,26.83mmstb, 15.47mmstb,) respectively. The results of the petrophysical evaluation indicate significant accumulation of hydrocarbon suggesting that the field may be referred to as prospect.

(Ogbamikhumi and Aderibigbe, 2019) in their work “Velocity modelling and depth conversion uncertainty analysis of onshore reservoirs in the Niger Delta basin” studied the depth uncertainties associated with field development which is as a result of complexity of the subsurface, paucity of data, well ties, fault positioning, time to depth conversion. To manage this uncertainty, two velocity modelling techniques, polynomial method and V_0_k methods were employed to build velocity models for depth conversion Four reservoir levels at various depths were analysed for depth residual after the depth conversion to select the method which gives the least average residuals and standard deviation to employ for depth conversion. The result of the depth residual analysis shows that both methods show a depth uncertainty of less than 50ft at shallow reservoir levels below 9000ft. As depth increases, the polynomial methods derived

residuals becomes unreliable as it has a depth uncertainty of over 100ft compared to 11.65ft of the V_0_K method for the deeper MOT reservoir. This is expected because the polynomial method uses average velocities while the V_0_K method uses instantaneous velocities. Hence the V_0_K method gives reliable results at greater depth during depth conversion and should be preferably used for velocity modelling and depth conversion studies for the Niger Delta basin.

2.2 GEOLOGICAL SETTING OF THE STUDY AREA

2.2.1 GEOLOGIC FRAMEWORK OF THE NIGER DELTA BASIN

The Niger Delta is one of the world's largest tertiary delta systems and is situated on the West African continental margin at the apex of the Gulf of Guinea (Doust and Omatshola, 1990). The Niger Delta basin extends over an area of 75,000 km² (Sonibare et al., 2008). It was formed during the continental rifting episode during the cretaceous era, with the delta developing from Paleocene. The lithostratigraphic sequence of the Niger Delta is divided into three formations. The Akata formation (Paleocene to Recent), the base of the delta, consists of thick shale deposited under marine conditions. The overlying Agbada Formation (Eocene into the Recent) consists of inter-bedded shale and sands and is overlain by the Benin formation (latest Eocene to Recent), which is composed of coastal plain sands (Sonibare et al., 2008; Short and Stauble, 1967). The source rocks for hydrocarbon in the Niger Delta are the marine shale facies of upper Akata formation and the paralic facies of shale interbedded with sands of the lower Agbada Formation. One petroleum system has been identified in the Niger Delta basin referred to as the tertiary Niger Delta (Akata – Agbada) petroleum system (Tuttle et al., 1999).

2.2.2 TECTONIC AND STRUCTURAL SETTING OF THE NIGER DELTA BASIN

The evolution of Niger Delta basin is related to the periods of rifting and later drifting of the African plate from the South American plate which led to the opening of the South Atlantic Ocean (Reijers et al., 1997). This rifting started and continued from the late Jurassic till mid Cretaceous and the rifting episode is diminished in Late-Cretaceous (Lehner and De Ruiter, 1977). After the Atlantic forming Mesozoic rift, sedimentation started with the Albian deposits. The Benue trough was filled with sediments and during the Late Eocene, the basin started prograding into the current continental slope and down to the deep sea. Continuous progradation of marine sediments since the Eocene extended to the current continental margin. Cretaceous

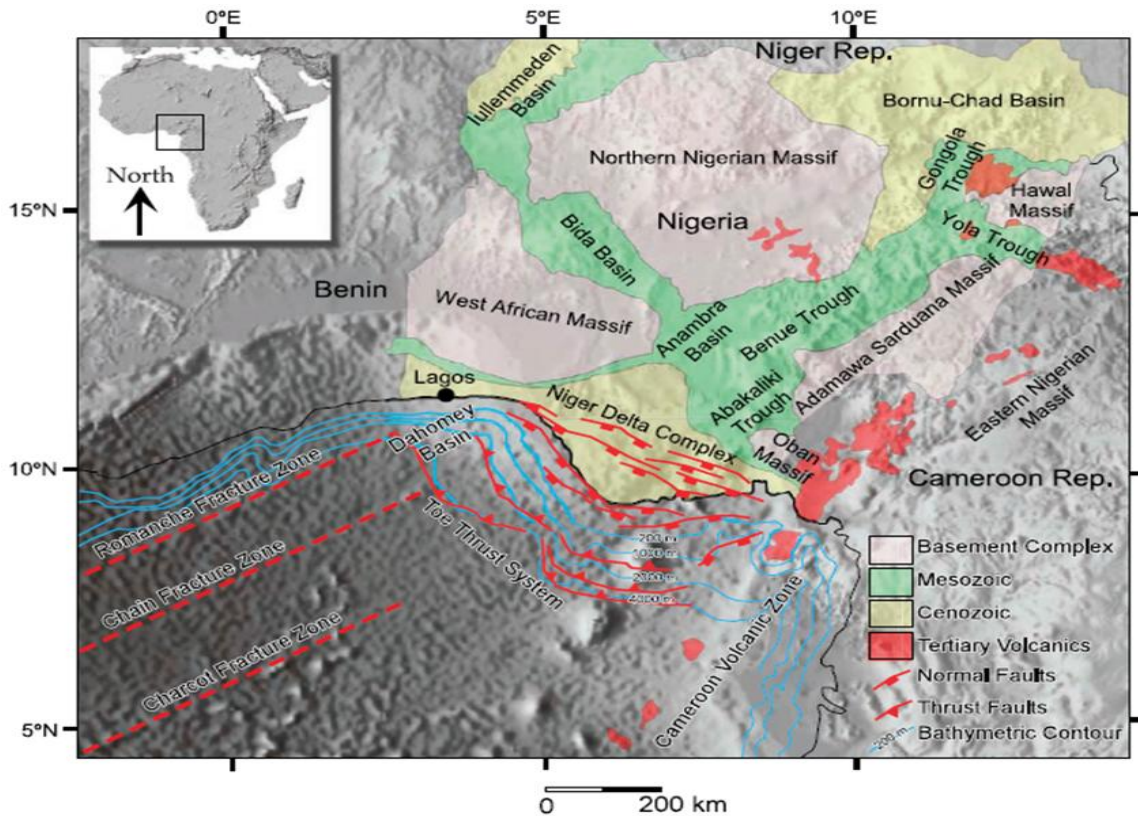


Figure 3: Map of Nigeria showing the Niger Delta complex (Whiteman, 1982).

fracture zones occurring as trenches and ridges in the abyssal plains of the Atlantic Ocean controlled the structural framework of the Niger Delta (Dim and Onuoha, 2017). The ridges subdivided the continental margin of the South Atlantic Ocean into separate basins, forming the Cretaceous Benue-Abakaliki trough's border faults and cutting far into the West African shield. The trough is a detached segment of a triple rift junction linked to the evolution of the South Atlantic Ocean.

The Niger Delta Basin extends from the south-facing coast of West Africa into the Benue Valley to the east (North, 1985). A triple junction has been proposed to have developed at the position of what is now the outer Niger Delta. The failed arm of the triple junction is the Anambra-Benue trough where oceanic crust failed to develop. The African and South American continents drew apart along the ridge—transform system of the Gulf of Guinea and South Atlantic arms of the junction. The rivers flowing along the Benue-Anambra failed arm disgorged into a regional down warp of the oceanic crust in the area of the triple junction. The tectonic framework of the continental margin along the West coast of equatorial Africa is controlled by cretaceous fracture

zones expressed as trenches and ridges in the deep Atlantic. The Pre-Tertiary structural framework controlled the direction and position of the progradational sediment fill. As the pre Tertiary structural depression was filled, the depositional centres moved seawards in consequence and the coastal plain deposits became progressively younger in that direction. The delta progrades over the narrow continental shelf and beyond the continental margin. During Oligocene-Miocene, the Delta complex had prograded southwards into deep waters and out onto the rapidly subsiding oceanic crust. (Nton and Adeyemi, 2021).

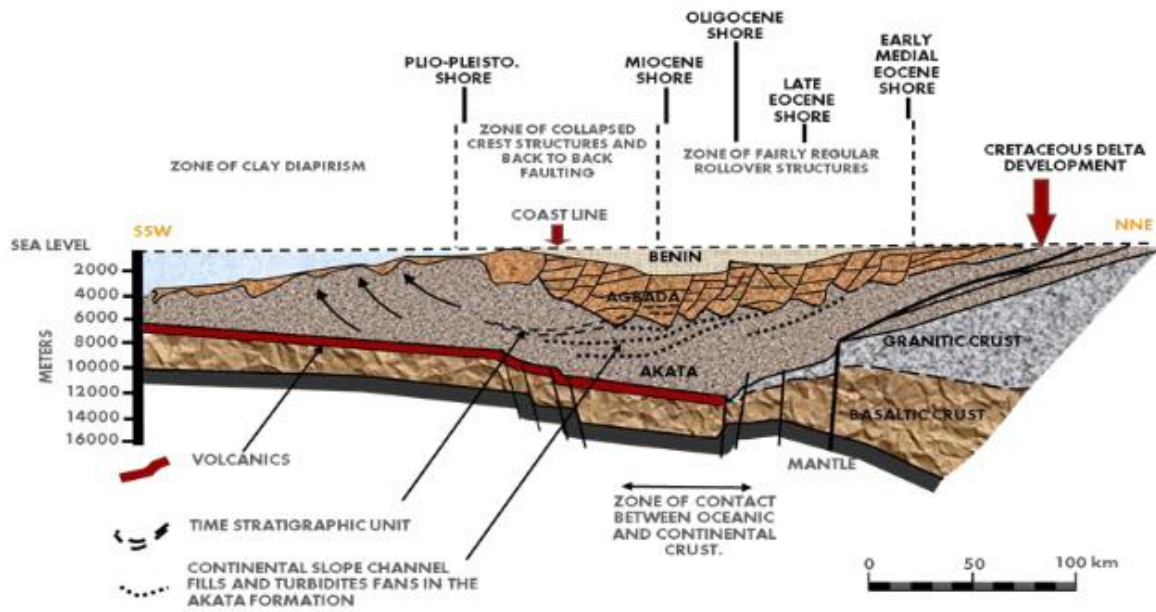


Figure 4: Schematic diagram of a dip section from the Niger Delta basin showing the various tectonic and structural elements. (Weber and Daukoru, 1975).

The tectonic structures in the Niger Delta Basin are very typical of an extensional rift system, but the added shale diapirism due to compression makes this basin different. The main method of deformation is due to shale gravitational tectonics within the basin, although the older faulting and deformation in the basin are related to the continental breakup and rifting of the African plate and South American plates. The overall basin is divided into different zones due to its tectonic structure. There is an extensional zone, which lies on the continental shelf that is caused by the thickened crust. There is a transition zone, and then there is a contraction zone, which lies in the deep waters part of the basin. Basin Inversion is caused by uplift and/or compression in

this basin. The compression is caused by the toe detachment of the shale diapirs. (Emujakporue et al., 2019).

(Evamy et al., 1978) described the major structural features of the Niger Delta as growth faults and rollover anticlines. A growth fault is a fault that offsets an active plain of deposition. It is usually syn-depositional. Generally the down thrown blocks have thicker sediments relative to the up thrown blocks. Theoretical calculations and field observations show that growth faults have a dip of 55 degrees or more near the surface (Anderson, 1942). Most of the oil accumulated in the Niger Delta is contained in the rollover anticline structure. The oil in these structures may be trapped in dip closures or against a Synthetic or antithetic fault. Growth faults are the most common subsurface structures in the Niger Delta.

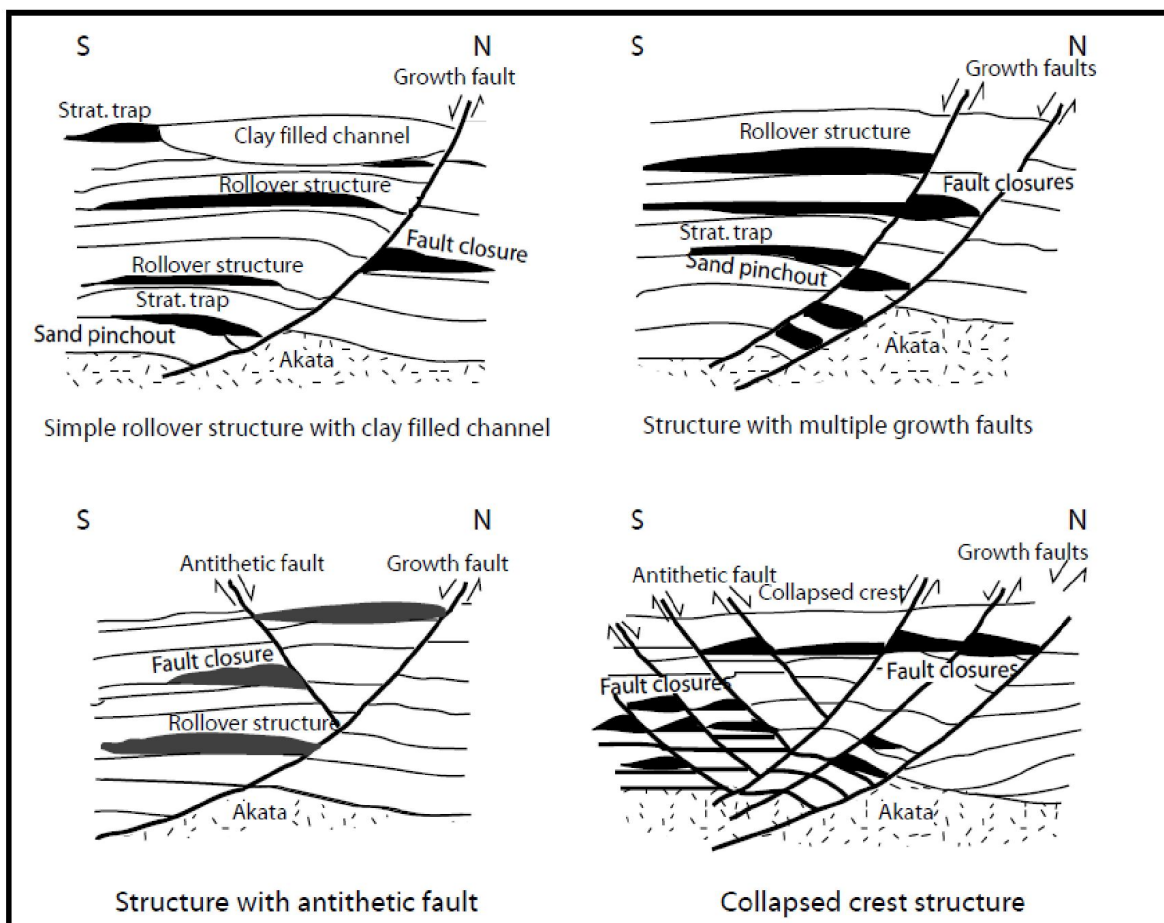


Figure 5: Niger Delta basin structures and associated trap types. (Modified from Doust and Omatsola, 1990; Stacher, 1995).

2.2.3 SEDIMENTARY FILL OF THE NIGER DELTA BASIN

The Niger delta is formed by tertiary sediments deposited in a high-energy constructive deltaic environment. The sedimentary fill in the Niger Delta basin is characterized by three diachronous lithostratigraphic units that range from the Palocene to Recent. These three lithostratigraphic units shows that the basin experienced an overall regression through time as the sediments progress from marine mudstones and shales to fluvial denser sand sized grains. The sediments came from the drainage system of River Niger, River Benue and Cross River. However, the delta is presently a complex river-marine system that followed a fashionable stage as the delta progressed southwest, forming several depobelts which represent the most active part delta in each depositional phase (Bowen et al., 1994).

a) DEPOBELTS

The deposition of the three formations occurred in each of the five off lapping cycles of siliciclastic sedimentation that make up the Niger Delta. These cycles (depobelts) are 30-60 kilometres wide, and prograde south-westward 250 kilometres over the oceanic crust into the Gulf of Guinea (Stacher, 1995), and are defined by syn-sedimentary growth faults that occurred in response to varying rates of subsidence and sediments supply (Doust and Omatsola, 1990). The interplay of subsidence and supply rates resulted in deposition of discrete depobelts-- when further crustal subsidence of the basin could no longer be accommodated, the focus of sediment deposition shifted seaward, forming a new depobelt (Doust and Omatsola, 1990). Each depobelt is a separate unit that corresponds to an interruption in the regional delta valley and is bounded landward by growth faults and seaward by large counter-regional faults or growth fault of successive seaward belt (Evamy et al., 1978; Doust and Omatsola, 1990). Five major depositional belts are generally recognized, each with its own sedimentation, deformation and petroleum history. (Doust and Omatsola, 1990) describe three structure-based depobelt provinces. The Northern Delta depobelt, which overlies relatively shallow basement, has the oldest growth faults which are generally rotational, equidistant and increase their slope towards the sea. The Central Delta depobelt has well-defined structures such as successively deeper rollover anticlinal crests that shift seaward for any given growth fault. Lastly, the distal delta depobelt is the most structurally complex due to internal gravity tectonics on the modern continental slope. These depobelts formed when paths of sediment supply were restricted by patterns of structural

deformation, focusing sediment accumulation into restricted areas on the delta. These depobelts changed position over time as local accommodation was filled and the locus of deposition shifted basin-ward. (Doust and Omatsola, 1990).

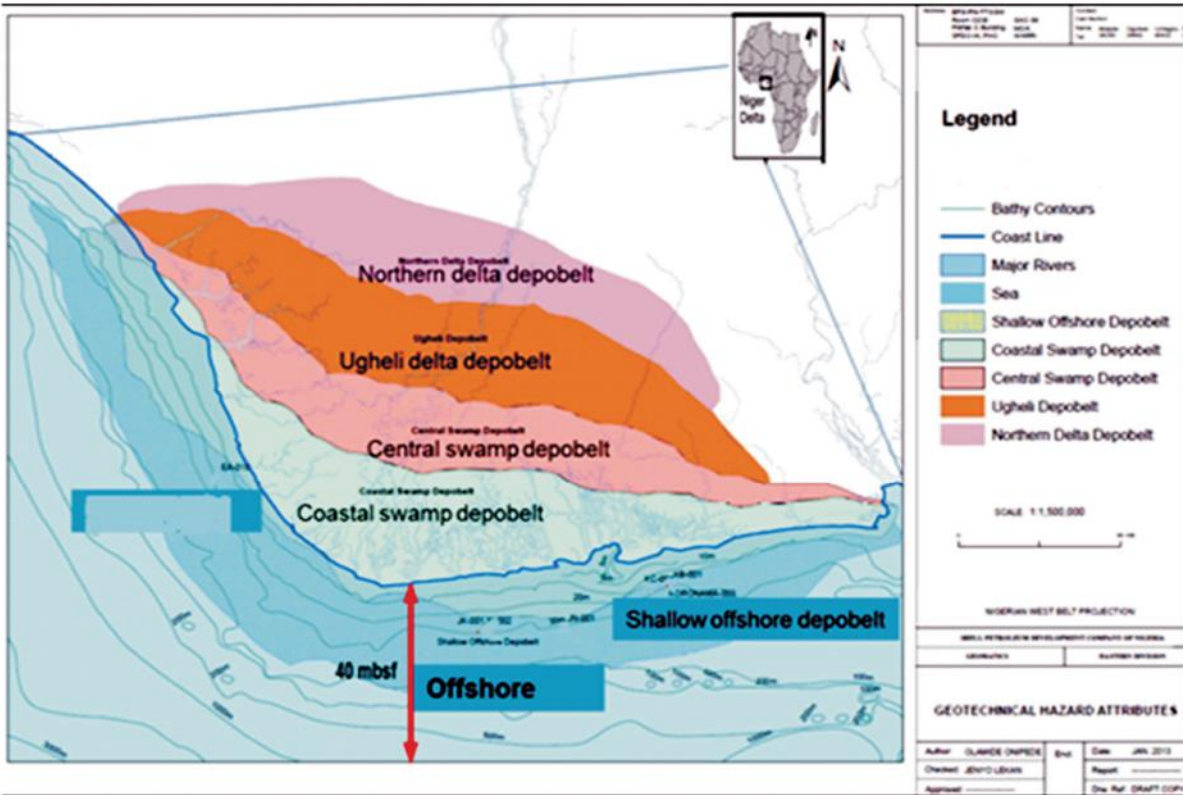


Figure 6: The map view of the different Depobelts in the Niger Delta (Nwozor et al, 2013)

2.2.4 STRATIGRAPHY OF THE NIGER DELTA

(Short and Stable, 1967) described the lithostratigraphy of Niger Delta as being made up of three formations; pro-delta shales (Akata Formation), overlain by interbedded delta front sands and shales (Agbada Formation), in turn, overlain by fluvial sands (Benin Formation). These deposits range in age from Palocene to Recent. These three geological formations of the Niger Delta are described below:

a) Benin Formation

The Benin Formation is the youngest and topmost lithostratigraphic unit of the Niger Delta basin, it has been described as the Coastal Plain Sands which outcrop in Benin, Onitsha and Owerri areas and elsewhere in the delta area. It consists of massive continental (non-marine) sands and

gravels considered to have been deposited in the alluvial or upper coastal plain environment. Very little to no hydrocarbons has been found in the Benin Formation (mainly due to lack of traps). The formation is generally water bearing, thus the main source of potable ground water in the Niger Delta area (Asadu et al., 2015). The first marine foraminifera located within shales indicate the base of the Benin Formation, as the formation is non-marine in origin (Short and Stauble, 1967).

b) Agbada Formation

The Agbada Formation overlies the Akata Formation and forms the middle lithostratigraphic units of the Niger Delta basin. This formation forms the hydrocarbon-prospective sequence in the Niger Delta. It is considered as the principal reservoir of Niger Delta hydrocarbon province, the formation has been studied in some detail. The Agbada Formation occurs as an intercalation of sands (fluvial, coastal, fluvio-marine), silts, clays, and marine shales (shale content increasing with depth) in various proportion and thicknesses, representing cyclic sequences of offlapping units. These paralic clastics are the true deltaic portion of the sequence and were deposited in a number of delta-front, delta-topset, and fluvio-deltaic environments and range in age from Eocene to Pleistocene (Doust and Omatsola, 1990).

c) Akata Formation

The Akata Formation is the basal unit of the Tertiary Niger Delta complex. This lithofacies is composed of shales, clays, and silts at the base of the known delta sequence. They contain a few streaks of sand, possibly turbidites (Asadu et al., 2015; Doust and Omatsola, 1990), and were deposited in holomarine (delta front to deeper marine) environments. The thickness of this sequence is not known for certain but may reach 7000m in the central part of the delta. Marine shales form the base of the sequence in each depobelt and range from Paleocene to Holocene in age (Asadu et al., 2015).

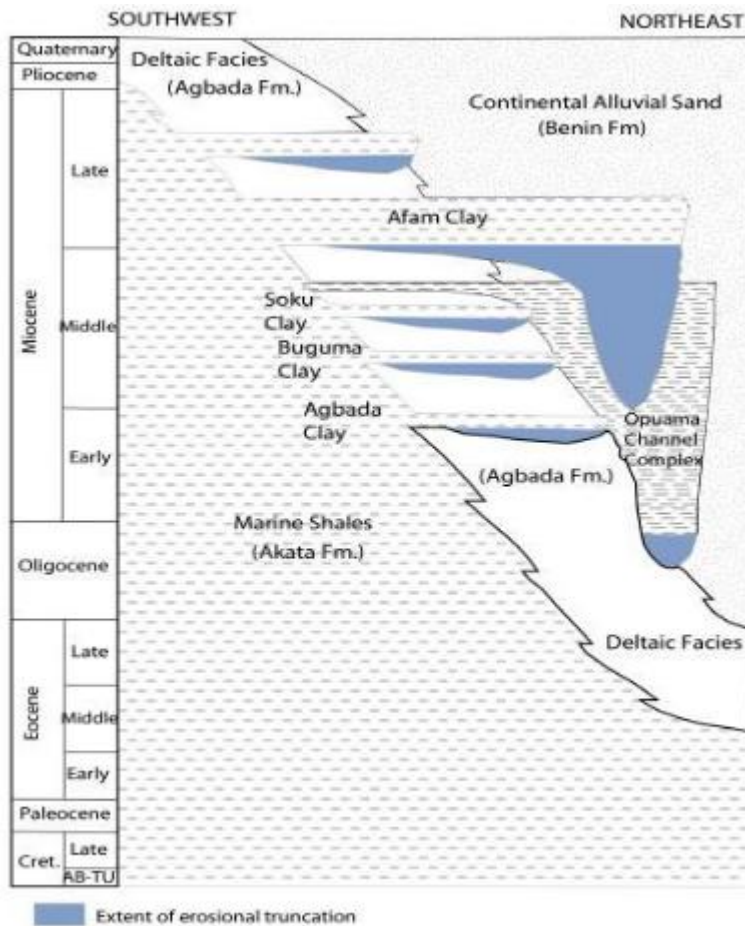


Figure 7: Stratigraphic column showing the three formational units of the Niger Delta. Modified from (Shannon and Naylor, 1989) and (Doust and Omatsola, 1990).

2.2.5 HYDROCARBON OCCURRENCE

Hydrocarbons occur within the Agbada formation of the Niger Delta. However, several directional trends form an “oil-rich belt” having the largest field and lowest gas/oil ratio (Ejedawe, 1981; Evamy et al., 1978; Doust and Omatsola, 1990). The belt extends from northwest offshore area to southeast offshore and along a number of north-south trends in the area of Port Harcourt. It roughly corresponds to the transition between continental and oceanic crust, and is within the axis of maximum sediment thickness. (Ejedawe, 1981) states that the two factors controlling the distribution of petroleum are; an increase geothermal gradient relative to the minimum gradient in the delta centre and the general older age of sediments within the belt relative to those further seaward. (Weber, 1987) indicates that the oil-rich belt (“golden lane”) coincides with a concentration of rollover anticlinal structures across depobelts having short

southern flanks and little parallel sequence to the south. (Doust and Omatsola, 1990) suggest that the distribution of petroleum is likely related to heterogeneity of source rock type (greater contribution from parallel sequences in the west) and/or segregation due to remigration.

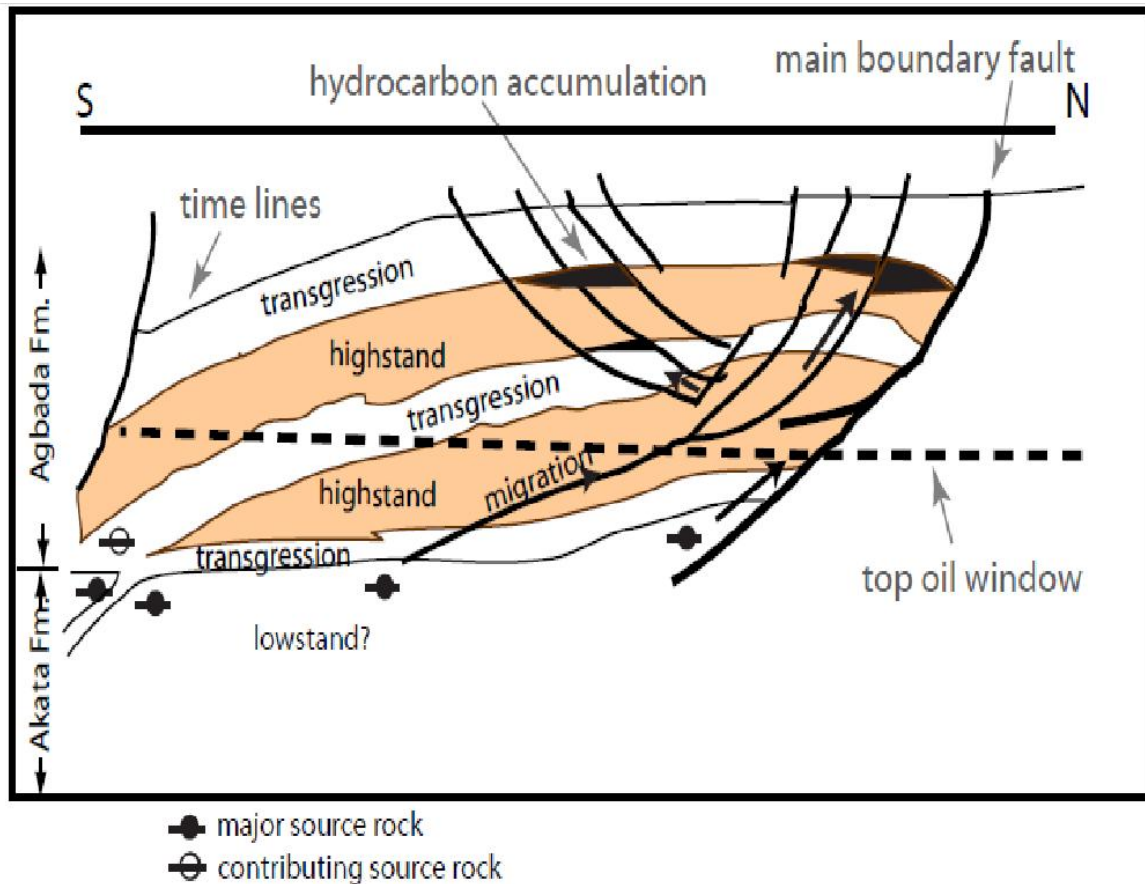


Figure 8: Sequence stratigraphic model of the central portion of the Niger Delta showing the relationship between the source rock, migration pathways and hydrocarbon traps related to growth faults (Modified from Stacher, 1995).

a) HYDROCARBON GENERATION

Hydrocarbons are compounds formed as result of breakdown of organic matter deposited with sediments in a reducing environment, from its original state to kerogen and then to hydrocarbon under the right temperature, pressure, and chemical conditions. (Evamy et al.,1978) set the top of the present-day oil window in the Niger Delta at the 240°F (115° C) isotherm. In the northwestern portion of the delta, the oil window (active source-rock interval) lies in the upper

Akata formation and the lower Agbada formation, to the southeast, the top of the oil window is stratigraphically lower (up to 1220 m) below the upper Akata/lower Agbada sequence. Although there are arguments over the effects of the ratios of sand/shale overburden on the depth to top of the oil window, it is believed that the depth increases southwards as reported (Beka and Oti, 1995). The process through which hydrocarbons migrate from the source to reservoir rocks was examined by (Hunt, 1990). He related this process to the case of the Gulf of Mexico under the assumption that the phenomenon is plausible in the Niger Delta. (Beka and Oti, 1995) predicted a bias towards lighter hydrocarbons (gas and condensate) from the over-pressured shale as a result of down-slope dilution of organic matter as well as differentiation associated with expulsion from over pressured sources.

b) SOURCE ROCK

Based on the volume, organic-matter content and type, the Akata shale is believed to be the source rock. However, there has been much discussion about the source rock for petroleum in the Niger Delta (Evamy et al., 1978; Ekweozor et al., 1979; Ekweozor and Okoye, 1980; Lambert-Aikhionbare and Ibe, 1984; Bustin, 1988; Doust and Omatsola,1990). Possibilities include variable contributions from the marine interbedded shale in the Agbada formation and the marine Akata shale, and Cretaceous shale (Weber and Daukoru, 1975; Evamy et al., 1978; Ekweozor and Okoye, 1980;Ekweozor and Daukoru, 1984; Lambert-Aikhionbare and Ibe, 1984; Doust and Omatsola,1990; Stacher, 1995; Frost, 1977; Haack et al., 1997).

The Agbada formation has intervals that contain organic carbon contents sufficient to be considered good source rocks (Ekweozor and Okoye, 1980; Nwachukwu and Chukwura, 1986). These intervals, however, rarely reach thickness sufficient to produce a world-class oil province and are immature in various parts of the delta (Evamy et al., 1978; Stacher, 1995). The Akata shale is present in large volumes beneath the Agbada Formation and is at least volumetrically sufficient to generate enough oil for a world class oil province such as the Niger Delta. Based on organic-matter content and type, (Evamy et al., 1978) proposed that both the marine shale (Akata formation.) and the shale interbedded with paralic sandstone (lower Agbada formation) are the source rocks for the Niger Delta.

c) MIGRATION

Migration from mature, over-pressured shales in the more distal portion of the delta may be similar to that described from over-pressured shales in the Gulf of Mexico. (Hunt, 1990) relates episodic expulsion of petroleum from abnormally pressured, mature source rocks to fracturing and resealing of the top seal of the over-pressured interval. In rapidly sinking basins, such as the Gulf of Mexico, the fracturing/resealing cycle occurs in intervals of thousands of years. This type cyclic expulsion is certainly plausible in the Niger Delta basin where the Akata Formation is over-pressured. (Beka and Oti, 1995) predict a bias towards lighter hydrocarbons (gas and condensate) from the over-pressured shale as a result of down-slope dilution of organic matter as well as differentiation associated with expulsion from over-pressured sources. This defines primary migration of hydrocarbons from the source rocks into the carrier beds.

Secondary migration is the movement of fluids, vertically and laterally within a porous reservoir or from one reservoir to another. In Niger delta, the best evidence for the vertical conductivity of major boundary faults is the fact that in most cases the fault intersection with the upper bedding plane of the reservoir functions as the spill point of the accumulation. At the level of the Akata formation, the major growth faults offset thicknesses up to several thousand meters of overpressured shale against paralic sediments in the downthrown block. A plausible migration pathway may thus be from the overpressured shale into and through the fault zone.

d) RESERVOIR ROCK

Petroleum in the Niger Delta is produced from sandstone and unconsolidated sands predominantly in the Agbada formation. Characteristics of the reservoirs in the Agbada Formation are controlled by depositional environment and by depth of burial (Tuttle et al., 1999). Known reservoir rocks are Eocene to Pliocene in age, and are often stacked, ranging in thickness from less than 15 meters to 45 meters thickness (Evamy et al., 1978). The thicker reservoirs likely represent composite bodies of stacked channels (Doust and Omatsola, 1990).

Based on reservoir geometry and quality, (Kulke, 1995) describes the most important reservoir types as point bars of distributary channels and coastal barrier bars intermittently cut by sand-filled channels. (Edwards and Santogrossi, 1990) describe the primary Niger Delta reservoirs as Miocene paralic sandstones with 40% porosity, 2 darcys permeability, and a thickness of 100 meters.

The lateral variation in reservoir thickness is strongly controlled by growth faults; the reservoir thickens towards the fault within the down-thrown block (Weber and Daukoru, 1975). The grain size of the reservoir sandstone is highly variable with fluvial sandstones tending to be coarser than their delta front counterparts; point bars fine upward, and barrier bars tend to have the best grain sorting. Much of this sandstone is nearly unconsolidated, some with a minor component of argillo-silicic cement (Kulke, 1995). Porosity only slowly decreases with depth because of the young sediments and the low temperature regime of the delta complex (Tuttle et al., 1999). In the outer portion of the delta complex, deep-water channel sands, low-stand sand bodies, and proximal turbidites create potential reservoirs (Beka and Oti, 1995).

e) TRAPS AND SEALS

Most known traps in Niger Delta fields are structural, although, stratigraphic traps are not uncommon (Figure 5). The structural traps developed during syn-sedimentary deformation of the Agbada Formation (Evamy et al., 1978; Stacher, 1995). The structural complexity increases from north (earlier formed depobelts), to the south (later formed depobelts) in response to increasing instability of the underlying over pressured shale. (Doust and Omatsola, 1990) describe a variety of structural trapping mechanisms, including those associated with simple rollover structures; clay filled channels, structures with multiple growth faults, structures with antithetic faults, and collapsed crest structures. The primary seal in the Niger Delta is the interbedded marine shale within the Agbada Formation. The shale provides three types of seals; clay smears along faults, interbedded sealing units against which reservoir sands are juxtaposed due to faulting, and vertical seals (Doust and Omatsola, 1990). On the flanks of the delta, major erosional events of early to middle Miocene age formed canyons that are now clay-filled. These clays form the top seals for some important offshore fields (Doust and Omatsola, 1990).

CHAPTER THREE

MATERIALS AND METHODOLOGY

3.1 MATERIALS

- i. A PC with Schlumberger Petrel software installed
- ii. 3D seismic data in SEG-Y format
- iii. Well log data

3.2 AVAILABLE DATA

The seismic data used was obtained from international oil company operating in Nigeria (Name withheld). Petrel software was used to load and interpret the seismic data. Other data provided were a suite of well logs and associated well log data such as checkshot data, well header and well deviation.

3.3 WORKFLOW

The processes involved in the completion of this project work are shown by the workflow in Figure 8 and further discussed in detail.

3.4 DATA LOADING AND QUALITY CHECK.

The available data sets were quality checked and loaded into the Petrel software for interpretation.

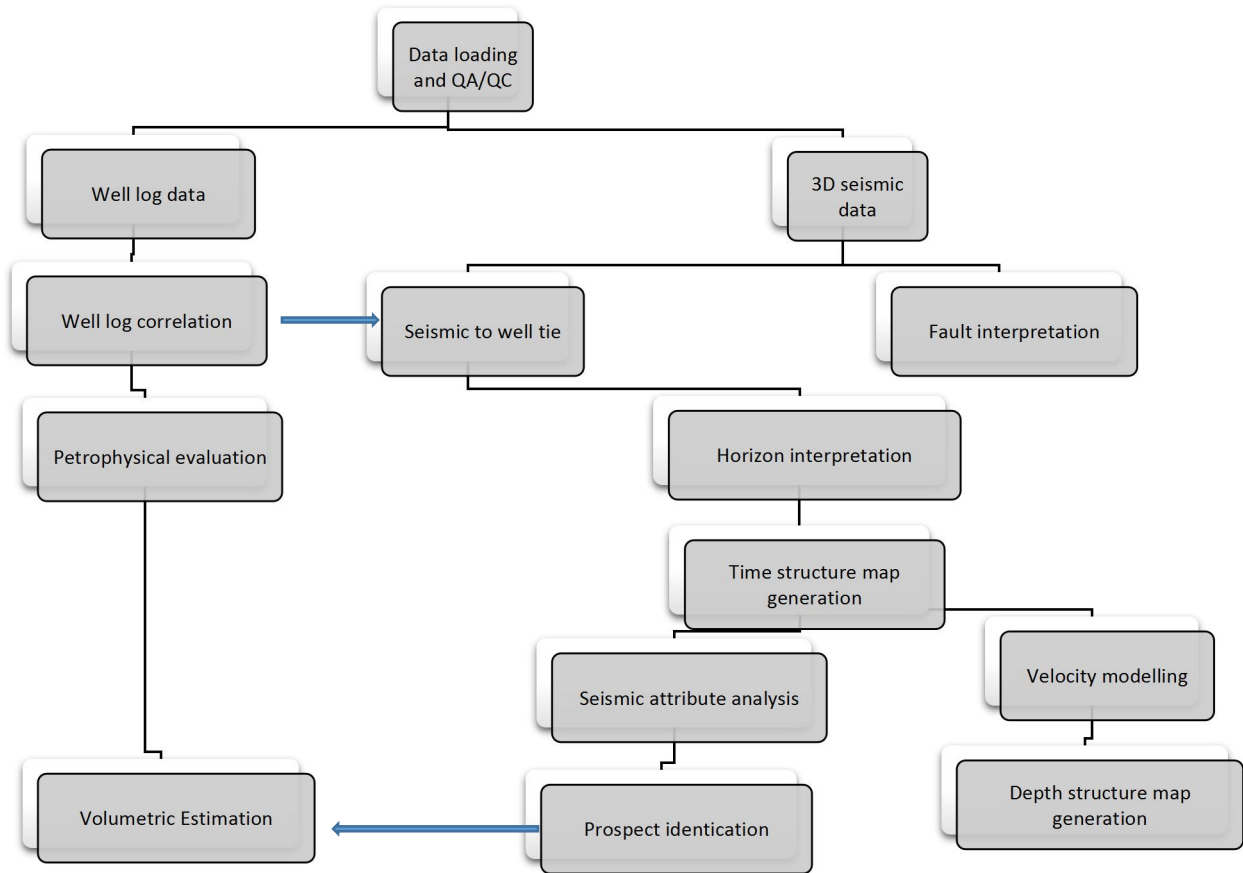


Figure 8: Workflow adapted

3.4.1 SEISMIC DATA

This 3D seismic data was acquired after seismic survey was carried out. This survey array arrangement allowed for the creation of several inlines and crosslines across the seismic data. The seismic data was loaded into the petrel software in SEG-Y format. The seismic data was needed to map faults which could serve as a trap for hydrocarbon accumulation and also to map horizons (reservoir tops) identified from the well logs (well to seismic tie) to create structural maps needed for hydrocarbon prospect identification. The loaded seismic is shown in figure 9.

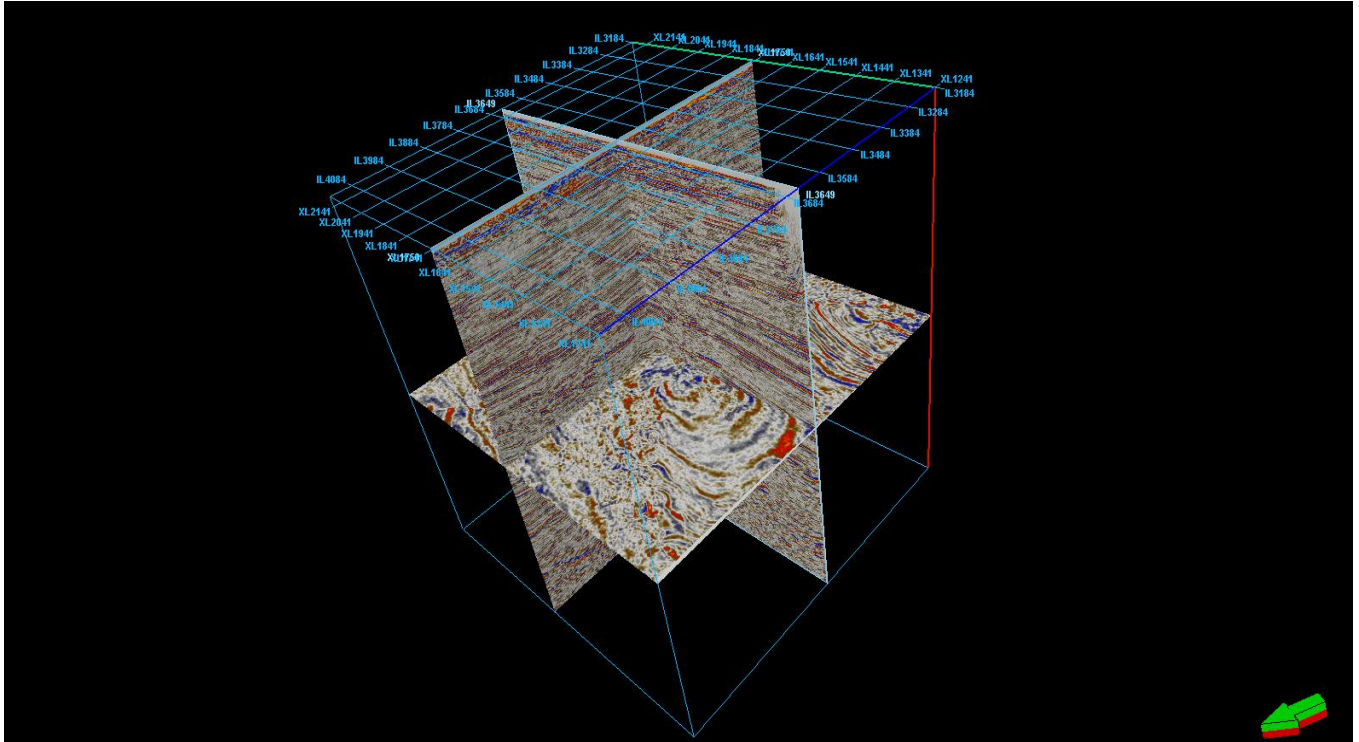


Figure 9: 3D view of study field when data was loaded.

3.4.2 WELL LOG DATA

This is information derived from the individual wells needed for evaluation. The well header contains individual well names, Surface X and Y coordinates, Kelly Bushing (a well reference datum), and Total depth (TD). The well deviation data provided was loaded into the software. A suite of 5 well logs; which consist of the gamma ray logs, resistivity logs, density log, sonic log and neutron porosity logs were loaded into the software in LAS format.

The check-shot data was loaded into the software in the ASCII format. It is used to create a relationship between the seismic (a function of time) and the well (a function of depth). It has a travel time that has been recorded at various depths in a well.

		Name	UWI	CALI	DENS	DTc	GR	NPHI	RESISTIVITY	SONIC	RES
1	<input checked="" type="checkbox"/>	AGBEJU 01		Yes	Yes	Yes	Yes	Yes	Yes	No	No
2	<input checked="" type="checkbox"/>	AGBEJU 02		Yes	Yes	No	Yes	Yes	No	Yes	Yes
3	<input checked="" type="checkbox"/>	AGBEJU 03		No	Yes	No	Yes	Yes	No	Yes	Yes
4	<input checked="" type="checkbox"/>	AGBEJU 04		Yes	Yes	No	Yes	Yes	No	Yes	Yes
5	<input checked="" type="checkbox"/>	AGBEJU X01		Yes	Yes	No	Yes	Yes	No	Yes	Yes

Figure 10: Available well logs

3.5 DATA INTERPRETATION

3.5.1 WELL LOG CORRELATION

Gamma ray logs are used for lithology identification. In the Niger Delta, we have siliciclastic sediments mainly sands and shale. They can be delineated on the gamma ray log based on natural radioactivity. Shales are more radioactive than sands due to their constituent radioactive minerals like thorium, uranium and potassium. Hence, the two lithologies can be differentiated on the gamma ray log with those having values greater than the cut off mark are regarded to as shale and those having values less than the cut off mark are regarded to as sands.

To establish the stratigraphic relationships between the lithofacies as well as the lateral distribution, we identify a key stratigraphic marker usually a continuous thick shale bed. This marker is integrated together with the motif of the sand bodies is used to correlate the sands across the wells.

After delineating all the potential reservoirs (sand bodies), the resistivity logs is used to delineate reservoirs which contain fluids with high resistivity values as hydrocarbon bearing reservoir(s). The neutron-density combination log is used to discriminate the fluid types (oil / gas) which can be found in the hydrocarbon bearing reservoir(s).

3.5.2 PETROPHYSICAL EVALUATION

Several petrophysical parameters are important in defining any reservoir, which include: shale volume (V_{sh}), total and effective porosity (Φ_{total} and Φ_{eff}), Net to Gross (NTG), permeability (K) and water saturation (SW).

a) Shale Volume (Vsh)

This is the clay content that is found within the reservoir rock. The volume of shale is determined from mathematical correlations and gamma ray index. The volume of shale is represented as Vsh. The gamma ray index (IGR) was first calculated in order to calculate the shale volume based on (Schlumberger, 1974) equation below

$$IGR = \frac{GR_{log} - GR_{min}}{GR_{max} - GR_{min}} \dots\dots\dots(Equation 1)$$

$$V_{sh} = 0.083 \times (2^{3.7 \times IGR} - 1) \dots\dots\dots(Equation 2)$$

Where;

IGR= gamma ray index

GR Log = log reading

GR min = minimum log value in clean sand and

GR max = maximum log value in 100% shale

b) Porosity (Φ)

Porosity is described as the percentage of the pore spaces to total volume of the rock.

Porosity is taken as the measure of the void space relative to the entire volume which shows the storage capacity of the given reservoir. Denoted by Phi (Φ). In measuring the total porosity, both the void spaces and the rock matrix are considered, regardless of whether effective or non-effective. The porosity was determined using the equation (Wyllie et al. 1958).

$$\Phi_{total} = \frac{\rho_{matrix} - \rho_{bulk}}{\rho_{matrix} - \rho_{fluid}} \dots\dots\dots(Equation 3)$$

Where;

Φ_{total} = total porosity

ρ_{matrix} = matrix density given as 2.65g/cm³

ρ_{bulk} = bulk density obtained from the density log

ρ_{fluid} = fluid density of water given as 1g/cm³

When the pore spaces are relatively connected then it is described as an effective porosity which accounts for the free-flowing fluid within a reservoir.

$$(\Phi_{eff}) = (1 - V_{sh}) \times \Phi_{Total} \dots\dots\dots(Equation 4)$$

Where;

Φ_{eff} = effective porosity

V_{sh} = volume of shale

Φ_{total} = total porosity

c) Net-To-Gross Ratio

This is measured as the potential productive part of a reservoir either as percentage producible (Net) part of the reservoir within the entire (Gross) reservoir or as a ratio.

$$NTG = (N/G) \times 100\% \dots\dots\dots(Equation 5)$$

Where;

NTG = Net to Gross

N = Net thickness

G = Gross thickness.

d) Permeability

In fluid flow, permeability tells the ease with which fluids flow through a porous medium. It is denoted by K and is expressed in Darcy or millidarcy. The permeability equation which is widely used in the Niger Delta in calculating the permeability for the reservoirs of interest was proposed by (Owolabi et al., 1994) and shown below;

$$K(mD) = 307+26552 \times (\Phi_{eff}^2) - 34540 \times (\Phi_{eff} \times S_{Wirr})^2 \dots\dots\dots(Equation 6)$$

Where;

K = permeability

Φ_{eff} = effective porosity

SW_{irr} = irreducible water saturation

$$SW_{irr} = (F/2000)^{0.5} \dots\dots\dots(\text{Equation 7})$$

Where F = formation factor

$$F = 0.62 / (\Phi_{Total}^{2.15}) \dots\dots\dots(\text{Equation 8})$$

e) **Water Saturation**

It is a pore volume occupied by formation water, expressed in either percentage or as a fraction. It is expected that water saturation should be equal to 1.

Water saturation is usually obtained using the Archie's formula (Archie, 1942)

given below :

$$SW = \frac{n \times a \times R_w}{\Phi_{total} \times m \times R_t} \dots\dots\dots(\text{Equation 9})$$

Where;

SW = Water saturation

n = Saturation exponent

Φ_{total} = total porosity

R_t = True Formation resistivity

m = Cementation exponent

a = Empirical constant

R_w = Resistivity of Formation water

3.5.3 WELL TO SEISMIC TIE

A synthetic seismogram was generated from the reference well by convolution of the reflection coefficient with a deterministic wavelet (Extended white wavelet) taken from the seismic volume. The reflection coefficient is calculated as a result of the acoustic impedance contrast between layers, where acoustic impedance is a product of the density and velocity. The velocity was determined from the sonic log which was calibrated with the checkshot data from the reference well.

To tie our well to seismic we highlight our reservoir tops and note the polarity of their reflection coefficient and adjust our synthetic seismogram to have the same polarity as the seismic data.

3.5.4 FAULT MAPPING

To understand the hydrocarbon-trapping mechanism, fault mapping is essential. The mapping of faults is most probably a distinct problem in seismic exploration. Faults are mapped on the dip lines (inlines) across the seismic sections. To understand the pattern of faults in the area of study, the fault trends are selected on several seismic inlines and mapped. When mapping faults, we employ the use of the Variance (edge) seismic attribute to guide the mapping exercise as it helps highlight the fault zones across the seismic volume.

3.5.5 HORIZON MAPPING

Horizons which correspond to the top of the reservoir(s) are best mapped on the strike line (cross lines) where they are more continuous with less truncation by faults. To interpret across the seismic data to give an idea of the structural framework of the identified horizon to help identify potential traps. Horizons are mapped across both the inlines and crosslines of the seismic data.

3.5.6 TIME STRUCTURAL MAP

Time structural maps were generated using the faults and horizons identified across the seismic data. Contouring was created by connecting points of equal time. The Time structural map represents the surface map of the reservoir(s) top and it shows the time taken for the incident acoustic energy to be hit and be reflected by the reflector to be recorded on the surface using a geophone / hydrophone.

3.5.7 DEPTH STRUCTURAL MAP

Depth structural maps were generated using the time to depth relationship gotten from the checkshot data. This results in the conversion of the time to distance hence the units of this map is no longer in time (ms) but have been converted to distance (ft). Contouring is created by connecting points of equal depth. The depth structural map represents the surface map of the reservoir top and it shows the distance of the reservoir top to the surface.

3.5.8 SEISMIC ATTRIBUTE ANALYSIS

With the aid of seismic surface attributes such as RMS amplitude, maximum amplitude, which act as direct hydrocarbon indicator (DHI). We can highlight areas within our time structural map where there is presence of hydrocarbon.

3.5.9 HYDROCARBON PROSPECT IDENTIFICATION

Potential hydrocarbon traps were identified from the contoured map of the horizons. Trap identification is based on contour values gotten from the surface and structural styles in association with the faults. It is a product of both fault and horizon interpretation. Prospects can be identified by integrating the result of the seismic attribute analysis and identified traps to highlight areas where significant hydrocarbon accumulations are trapped in commercial quantities.

3.5.10 VOLUMETRIC ESTIMATION

Volumetric estimation is calculated using results from the petrophysical evaluation and the area of the identified prospect. For the purpose of this work, GIIP and OIIP will be estimated.

- i. Calculation of Gas initially in place (GIIP)

$$GIIP = 43560 \times A \times h \times \Phi_{total} \times (1 - SW) \dots\dots\dots (Equation 10)$$

- ii. Calculation of Oil Initially In Place (OIIP)

$$OIIP = 7758 \times A \times h \times \Phi_{total} \times (1 - SW) \dots\dots\dots (Equation 11)$$

Where;

43560 = feet³ /acres-feet² conversion for gas

7758 = bbl /acres-feet² conversion for oil

A = Area in acres

h = Net Pay thickness in feet

Φ_{total} = Total porosity

SW = Water saturation

CHAPTER FOUR RESULTS AND DISCUSSION

4.1 RESULT AND DISCUSSION OF PETROPHYSICAL EVALUATION.

4.1.1 WELL LOG CORRELATION

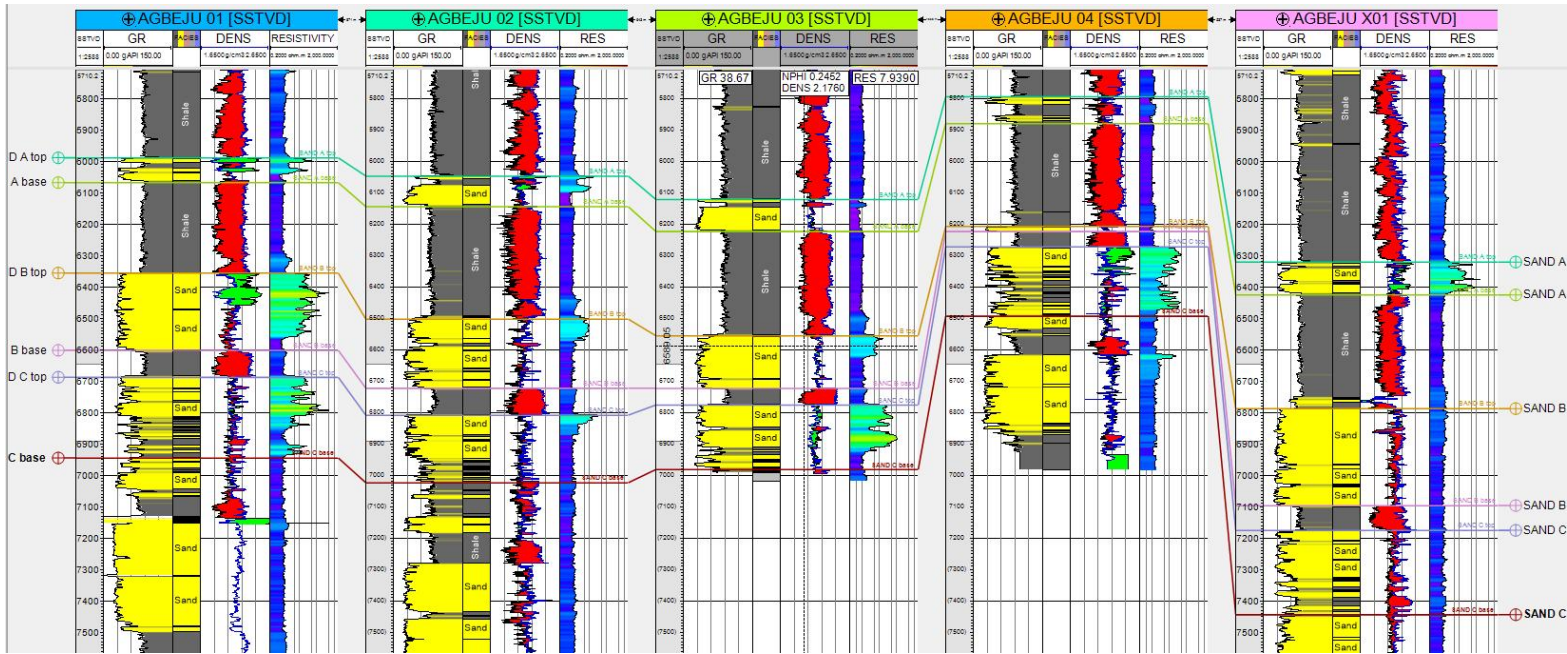


Figure 11: well correlation of the sand bodies across the wells on the well section window.

To carry out lithology correlation across the five wells (Agbeju 01, Agbeju 02, Agbeju 03, Agbeju 04 and Agbeju X01), we use a suite of well logs, gamma ray logs are used for lithology identification and correlation, where we first identify a marker shale bed and correlate the sand bodies above and below the shale marker bed. Using the configuration of the sand motif we can identify similar sand geometries across the wells and at variable depths. We correlate the sand bodies with similar motif across the well to define a continuous sand reservoir.

For hydrocarbon bearing sand reservoir delineation, we add the resistivity logs and the neutron porosity combination logs to the well section window. High resistivity values of fluids within the sand reservoirs indicate hydrocarbon presence. Wide separation of the neutron and density curves shows presence of gas while a closer separation between the curves shows presence of oil. Areas within the sand bodies that contain low resistivity values indicate water and define a fluid contact within the hydrocarbon bearing reservoir.

As a result of the well log correlation shown in figure 11 above, 3 hydrocarbon bearing reservoirs have been delineated and identified as Sand A, Sand B and Sand C.

4.1.2 PETROPHYSICAL EVALUATION

Quantitative interpretation which defines the petrophysical parameters of the delineated hydrocarbon bearing reservoir sands identified within the five wells (Agbeju 01, Agbeju 02, Agbeju 03, Agbeju 04 and Abeju X01) were used to evaluate the hydrocarbon potential of drilled part of Agbeju field. The summary of calculated petrophysical parameters through the analyses of available well log data are presented in Tables 1-3. Each of the tables presents the different petrophysical parameters obtained through the analyses of well logs from the three (3) hydrocarbon bearing reservoir identified in each well.

a) Petrophysical evaluation of Sand A

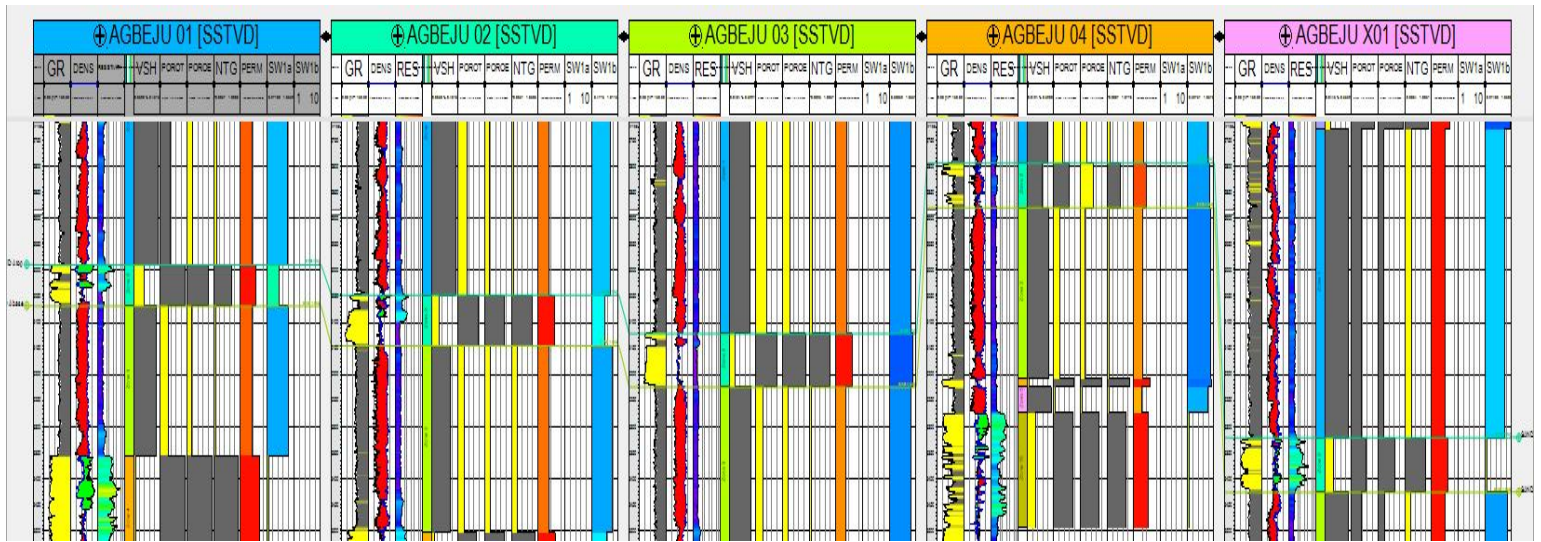


Figure 12: Correlation and petrophysical evaluation of sand A across the wells

Sand A was penetrated by all five (5) wells. The reservoir thickness ranges from about 85.79ft – 105.06ft m. Net to gross ranges from 0.4901 to 0.8805. The total porosity of Sand A ranges from 0.2439 to 0.3389.

Effective porosity ranges from 0.1752 to 0.2836. Permeability ranges from 864.24 to 1,700 mD. The summary of petrophysical evaluation is shown in the table 1 below.

From well correlation shown in figure 12 above, we identify hydrocarbons within wells Agbeju 01, Agbeju 02 and Agbeju X01. Within Agbeju 01, there is presence of gas with a gas water

contact at depth of 6039.72ft, water saturation of 0.609 and pay thickness of 48.52ft. Within Agbeju 02, there is presence of gas with gas water contact at depth of 6099.26ft, water saturation of 0.73478 and pay thickness of 51.33ft. Within Agbeju X01, there is presence of gas throughout the reservoir with water saturation of 0.33857 and pay thickness of 92.505ft.

Table 1: Petrophysical evaluation of Sand A

WELLS	TOP (ft)	BASE (ft)	GROSS THICKNESS	NTG	Vsh	Φ_{total}	Φ_{eff}
AGBEJU 01	5991.2	6068.94	77.74	0.7157	0.198	0.3389	0.2836
AGBEJU 02	6047.93	6144.58	96.65	0.8136	0.17	0.3145	0.2687
AGBEJU 03	6120.27	6223.57	103.3	0.8271	0.137	0.31	0.2757
AGBEJU 04	5794.6	5880.39	85.79	0.4901	0.3173	0.2439	0.1752
AGBEJU X01	6321.62	6426.68	105.06	0.8805	0.1408	0.3	0.2609
SW	PERM (mD)	NET THICKNESS	PREDICTED FLUID	FLUID CONTACT	PAY THICKNESS		
0.609	1,602.59	68.45007	GAS	GWC= 6039.72	48.52		
0.73478	1,618.50	78.63444	GAS	GWC= 6099.26	51.33		
0.97243	1700.96	85.43943	WATER	WUT	0		
0.90529	864.21	42.045679	WATER	WUT	0		
0.33857	1842.01	92.50533	GAS	GDT	92.50533		

GWC= gas water contact, GDT= gas down to, WUT= water up to.

b) Petrophysical evaluation of Sand B

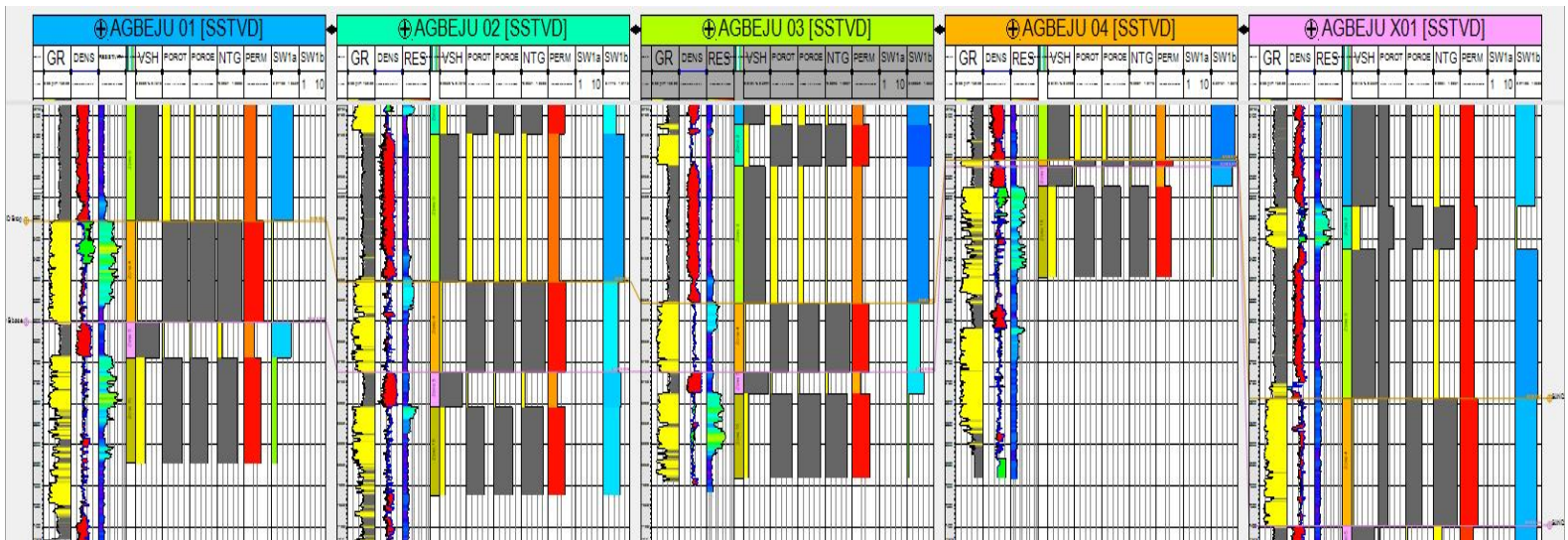


Figure 13: Correlation and petrophysical evaluation of Sand B across the wells

Sand B was penetrated by all five (5) wells. The reservoir thickness ranges from about 15.76ft – 243.38ft m. Net to gross ranges from 0.9247 to 1. The total porosity of Sand A ranges from 0.2685 to 0.3386. Effective porosity ranges from 0.249 to 0.3139. Permeability ranges from 1858.71 to 2,739.92 mD. The summary of petrophysical evaluation is shown in the table 2 below. From well correlation shown in figure 13 above, we identify hydrocarbons within wells Agbeju 01, Agbeju 02 and Agbeju 03. Within Agbeju 01, there is presence of gas and oil with a gas oil contact at depth of 6459.98ft and oil water contact at depth of 6563.25, water saturation of 0.337 and pay thickness of 206.61ft. Within Agbeju 02, there is presence of oil with oil water contact at depth of 6573.76ft, water saturation of 0.76746 and pay thickness of 68.29ft. Within Agbeju 03, there is presence of oil with oil water contact at depth of 6624.53ft, with water saturation of 0.70799 and pay thickness of 68,28ft

Table 2: Petrophysical evaluation of Sand B

WELLS	TOP (ft)	BASE (ft)	GROSS THICKNESS	NTG	Vsh	Φ_{total}	Φ_{eff}
AGBEJU 01	6356.64	6600.02	243.38	1	0.742	0.3386	0.3139
AGBEJU 02	6505.47	6724.33	218.86	0.9406	0.1106	0.2985	0.2683
AGBEJU 03	6556.25	6724.33	168.08	0.9884	0.0805	0.2698	0.249
AGBEJU 04	6207.81	6223.57	15.76	0.9247	0.083	0.2846	0.2656
AGBEJU X01	6787.37	7097.28	309.91	0.9935	0.0701	0.2695	0.2511
SW	PERM (mD)	NET THICKNESS	PREDICTED FLUID	FLUID CONTACT		PAY THICKNESS	
0.33709	2739.92	243.38	GAS AND OIL	GOC= 6459.98, OWC= 6563.25		206.61	
0.76746	1940.15	205.859716	OIL	OWC= 6573.76		68.29	
0.70799	1858.71	166.130272	OIL	OWC= 6624.53		68.28	
0.952	1764.09	14.573272	WATER	WUT		0	
0.86784	1896.11	307.895585	WATER	WUT		0	

GOC= Gas water contact, OWC= oil water contact, WUT= water up to

c) Petrophysical evaluation of Sand C

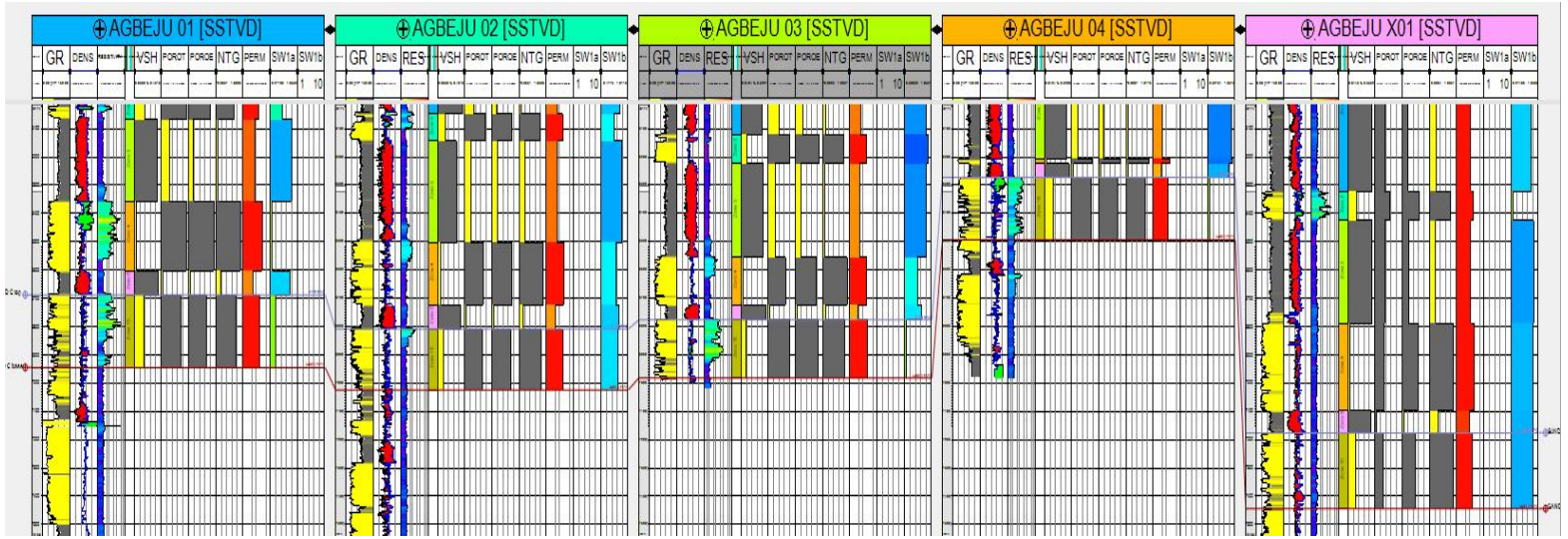


Figure 14: Correlation and petrophysical evaluation of sand C across the wells

Sand C was penetrated by all five (5) wells. The reservoir thickness ranges from about 204.86ft – 257.38ft m. Net to gross ranges from 0.7554 to 0.9769. The total porosity of Sand A ranges from 0.2617 to 0.3045. Effective porosity ranges from 0.2307 to 0.2676. Permeability ranges from 1233.17 to 1966.09 mD. The summary of petrophysical evaluation is shown in the table 3 below. From well correlation shown in figure 14 above, we identify hydrocarbons within wells Agbeju 01, Agbeju 02, Agbeju 03 and Agbeju 04. Within Agbeju 01, there is presence of oil with a oil water contact at depth of 6887.14ft, water saturation of 0.43025 and pay thickness of 199.57ft. Within Agbeju 02, there is presence of oil with oil water contact at depth of 6838.14ft, water saturation of 0.80648 and pay thickness of 28.01ft. Within Agbeju 03, there is presence of oil with oil water contact at depth of 6927,44ft, water saturation of 0.44556 and pay thickness of 148.83ft. Within Agbeju 04, there is presence of gas and oil with a gas oil contact at depth of 6328.91ft and oil water contact at depth of 6363.64.25, water saturation of 0.8805 and pay thickness of 91.04ft.

Table 3: Petrophysical evaluation of Sand C

WELLS	TOP (ft)	BASE (ft)	GROSS THICKNESS	NTG	Vsh	Φ_{total}	Φ_{eff}
AGBEJU 01	6687.57	6944.95	257.38	0.7905	0.18	0.3006	0.2503
AGBEJU 02	6810.13	7023.74	213.61	0.858	0.1446	0.295	0.2539
AGBEJU 03	6778.61	6983.47	204.86	0.8709	0.1282	0.3045	0.2676
AGBEJU 04	6272.6	6494.96	222.36	0.7554	0.1956	0.2766	0.2307
AGBEJU X01	7176.07	7443.96	267.89	0.9769	0.1299	0.2617	0.2314
SW	PERM (mD)	NET THICKNESS	PREDICTED FLUID	FLUID CONTACT		PAY THICKNESS	
0.43025	1653.5	203.45889	OIL	OWC= 6887.14		199.57	
0.80648	1794.65	183.27738	OIL	OWC= 6838.14		28.01	
0.44556	1966.09	178.412574	OIL	OWC= 6927.44		148.83	
0.38665	1233.17	167.970744	GAS AND OIL	GOC= 6328.91, OWC= 6363.64		91.04	
0.8805	1478.34	261.701741	WATER	WUT		0	

GOC= gas oil contact, OWC= oil water contact

4.2 RESULTS AND DISCUSSIONS OF 3D SEISMIC INTERPRETATION.

4.2.1 FAULT INTERPRETATION

A total of thirty three faults including 9 major faults and 24 minor faults were discovered to highlight the fault pattern in Agbeju field, the fault lines are selected on several seismic inlines and mapped until the trend ends. The Variance edge seismic volume attribute aided the fault mapping as it highlights fault zones across the seismic volume; this is highlighted in figure 15.

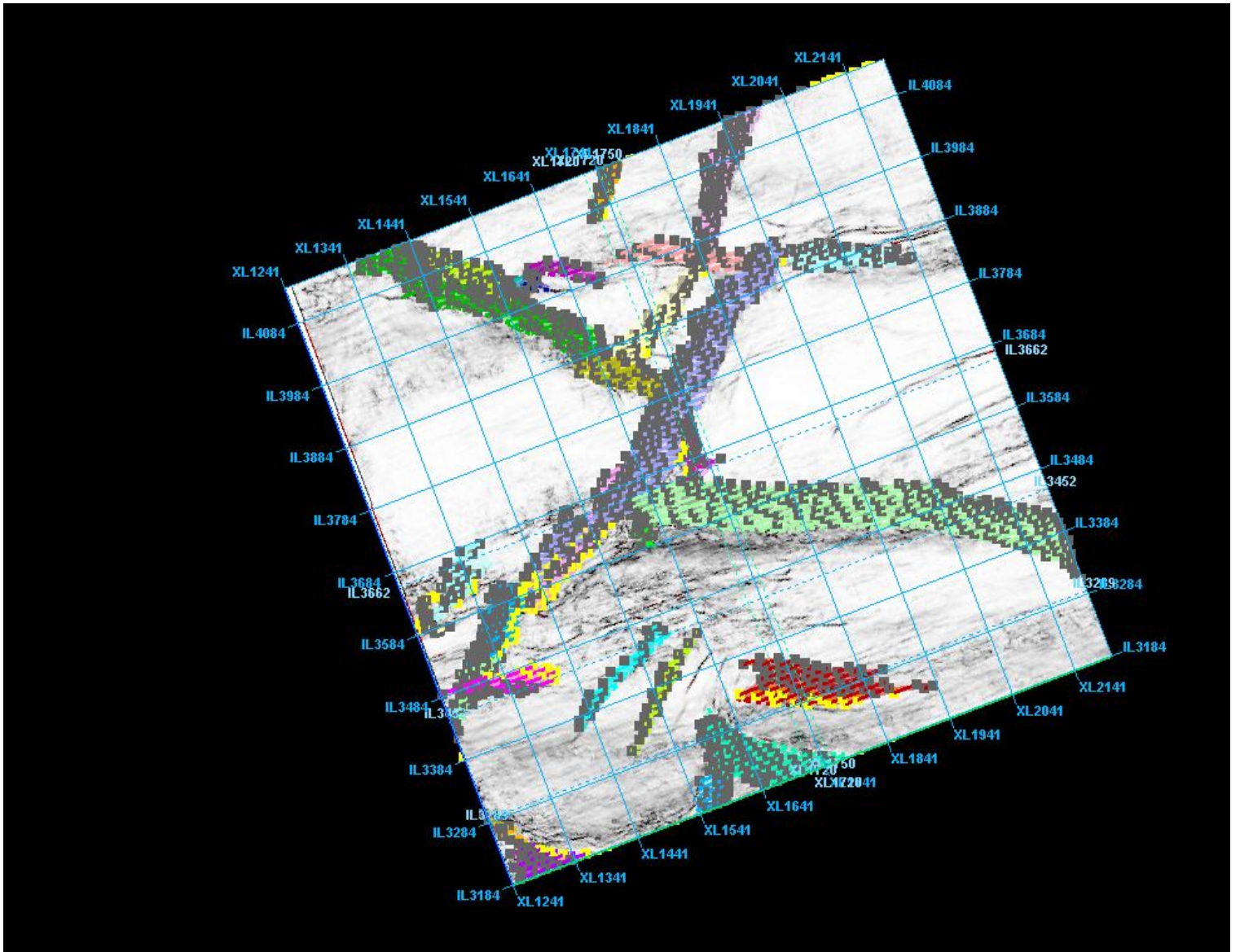


Figure 15: Faults shown on time slice of the variance edge seismic data

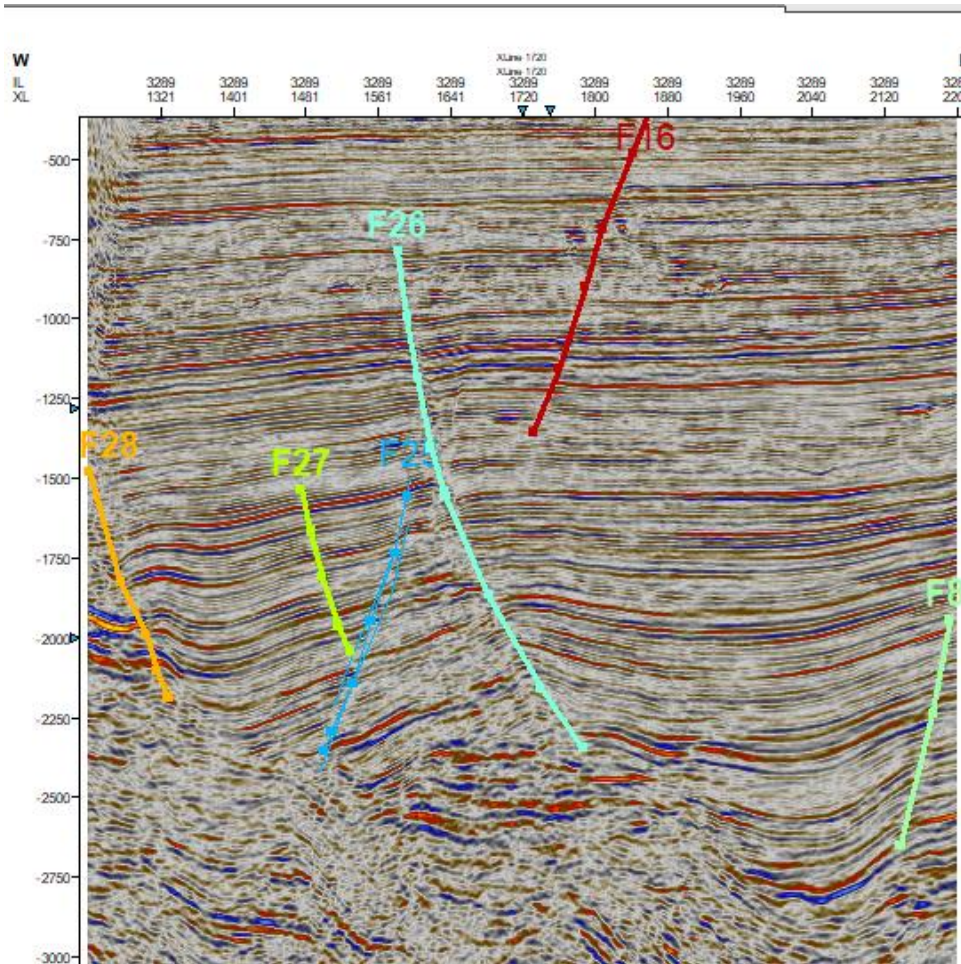


Figure 16: mapped faults along Xline on interpretation window.

4.2.2 WELL TO SEISMIC TIE

Well to seismic tie was conducted to convert our well log data into reflection coefficients and tie the position of our well onto the seismic data. A synthetic seismogram was generated from the Agbeju 02 by convolution of the reflection coefficient with a deterministic wavelet (Extended white wavelet) taken from the seismic volume. The reflection coefficient is calculated as a result of the acoustic impedance contrast between adjoining layers, where acoustic impedance is a product of the density and velocity. The velocity was determined from the sonic log which was calibrated with the checkshot data from the Agbeju 02. The well to seismic tie is shown in the figure 17 below.

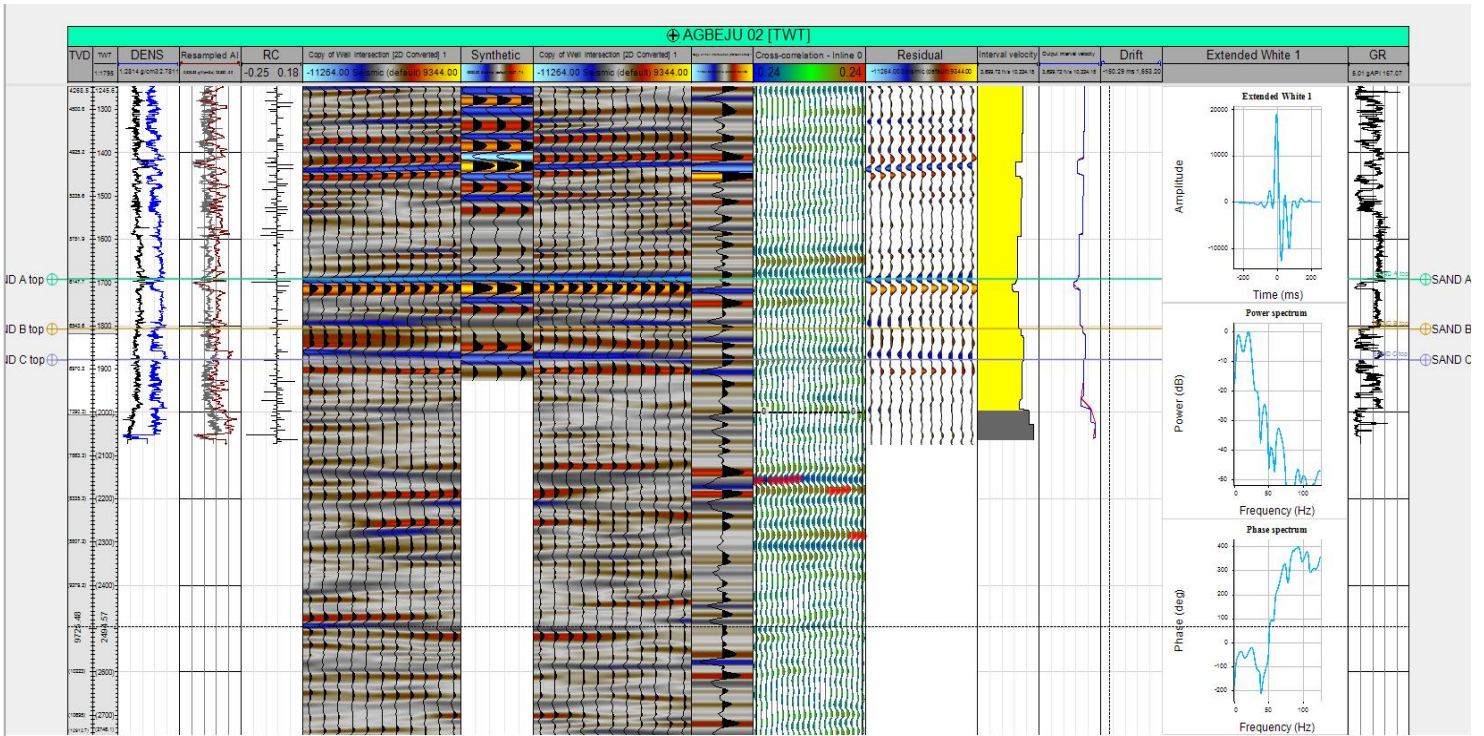


Figure 17: Seismic to well tie using Agbeju 02 well.

4.2.3 HORIZON INTERPRETATION

After the well to seismic tie, we identify the reflectors that represent the tops of Sand A, Sand B and Sand C, these three reflectors are then mapped across the seismic volume along the inlines and xlines interpretation windows. These horizons are identified in the figure 18 below as Horizon A, Horizon B and Horizon C.

In Figure 19 below, the horizons are shown fully mapped across both the inlines and xlines across the seismic data. These horizons are mapped along the seismic reflector which represents the top of the reservoir. The lateral extent of the horizons are shown in the map window. We have Horizon A in figure 19 (a), Horizon B in figure 19 (b) and Horizon C in figure 19 (c).

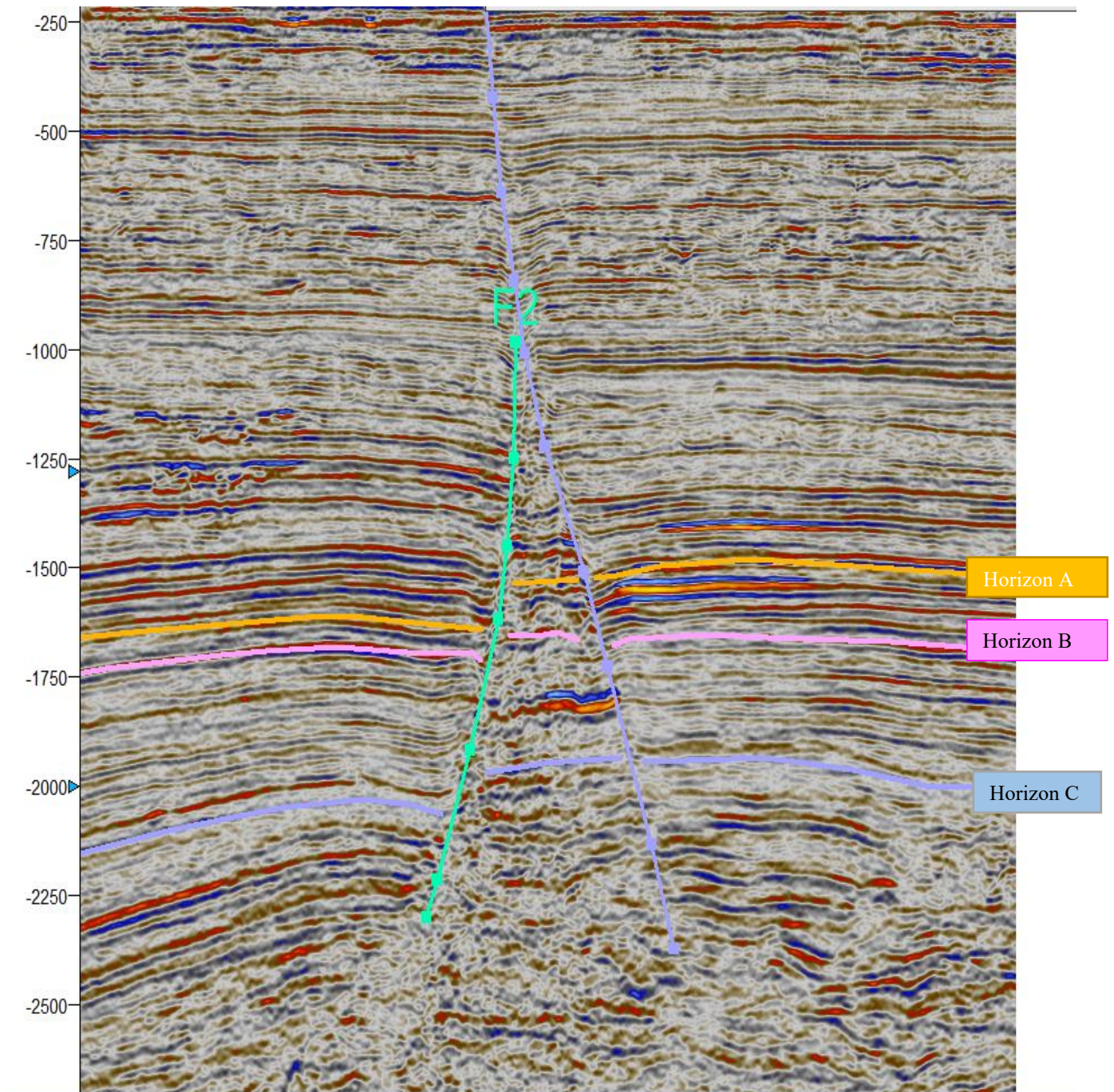


Figure 18: Horizon mapping along Xline on interpretation window showing faults and the three horizons (A, B, C).

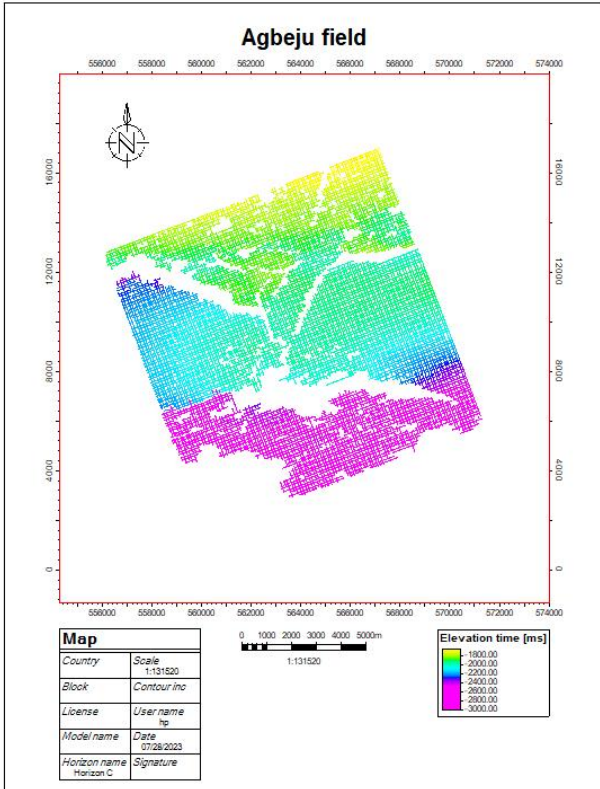
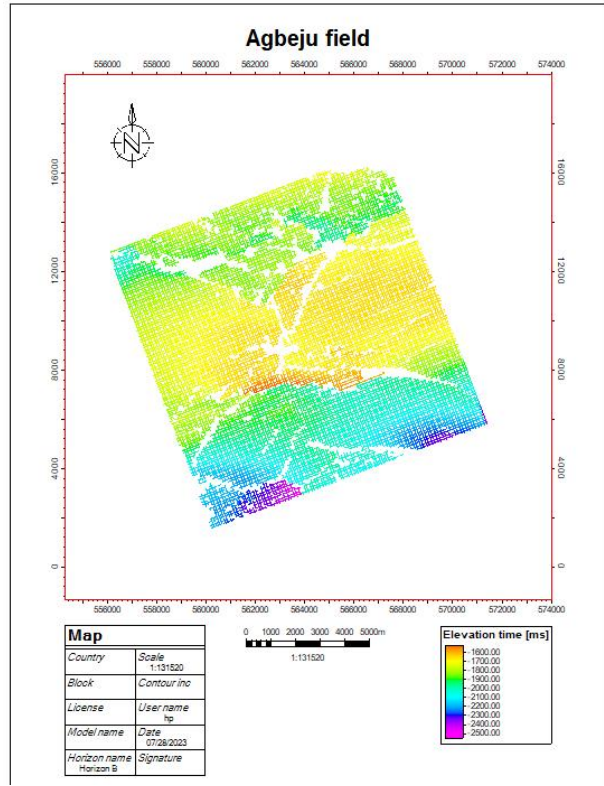
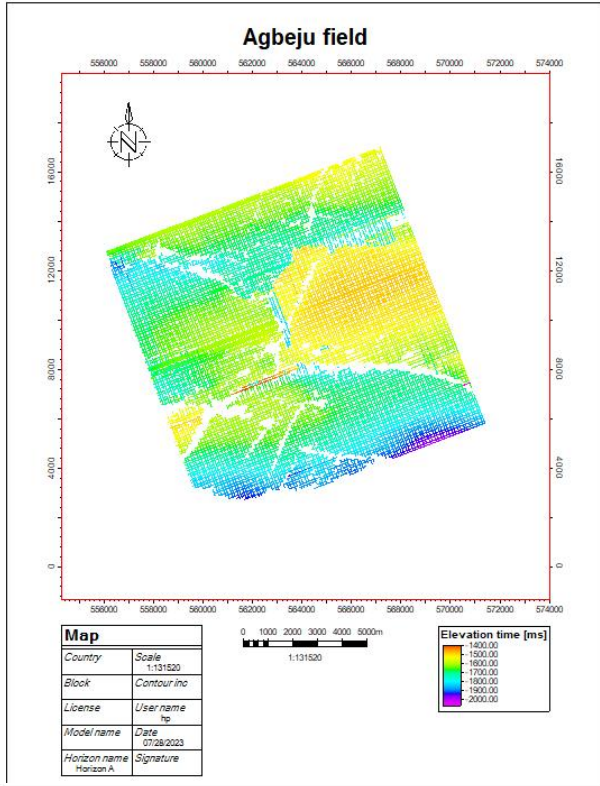


Figure 19: Horizons generated on map window with horizon A at top left, horizon B at top right and horizon C at bottom left.

4.2.4 TIME STRUCTURAL MAP

After the interpretation of horizon, a surface was generated with the use of the polygon editing to generate a boundary polygon around the horizon and fault polygons for each individual fault. Contours were generated and added to the surface.

The structural time map result for sand A is shown in figure 20(a). The time structure map shows contour intervals of 50 ms with contour values ranging from 1550ms to 1950ms. The colour legend shows differences in elevation (ms) on the map. The structural time map result for sand B is shown in figure 20(b). The time structural map shows contour intervals of 50 ms with contour values ranging from 1650ms to 2500ms. The colour legend shows differences in elevation (ms) on the map.

The structural time map result for sand C is shown in figure 20(c). The time structural map shows contour intervals of 50 ms with contour values ranging from 1700ms to 2900ms. The colour legend shows differences in elevation (ms) on the map.

4.2.5 DEPTH STRUCTURAL MAP

The depth structural map is generated from the time structural maps using the time – depth relationship derived from seismic to well tie. The third order polynomial function is used to model this relationship across the seismic data. The equation for Z_vs_TWT_picked is shown below.

$$y = 54.4516 + 2.1848 \times (x - 0.00126384) \times (x^2 - 2.50694E7) \times x^3 \dots\dots\dots \text{(Equation 12)}$$

The structural depth map result for sand A is shown in figure 21(a). The depth structural map shows contour intervals of 200 m with contour values ranging from 5200ft to 7200ft. The colour legend shows differences in elevation (ft) on the map.

The structural depth map result for sand B is shown in figure 21(b). The depth structural map shows contour intervals of 100 m with contour values ranging from 5850ft to 8050ft. The colour legend shows differences in elevation (ft) on the map.

The structural depth map result for sand C is shown in figure 21(c). The depth structural map shows contour intervals of 100 m with contour values ranging from 6250ft to 8050ft. The colour legend shows differences in elevation (ft) on the map.

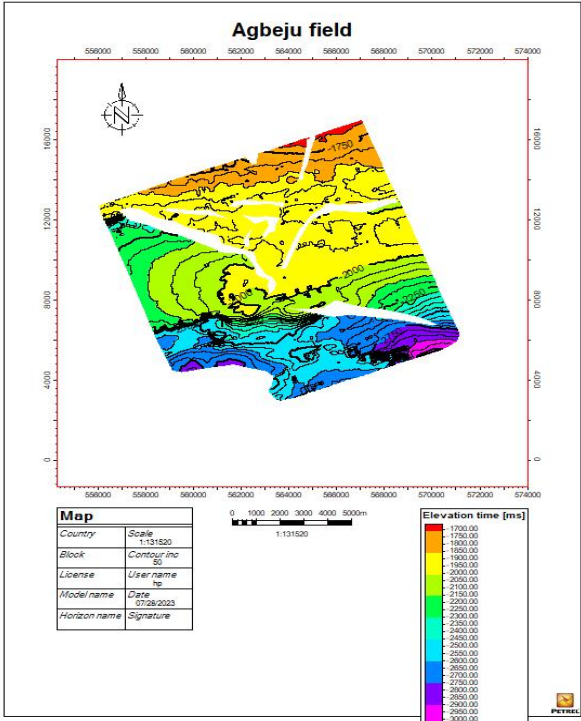
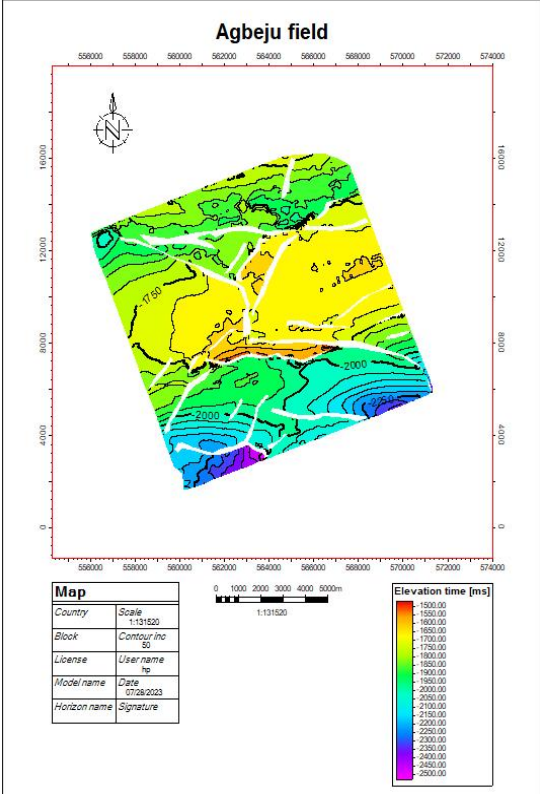
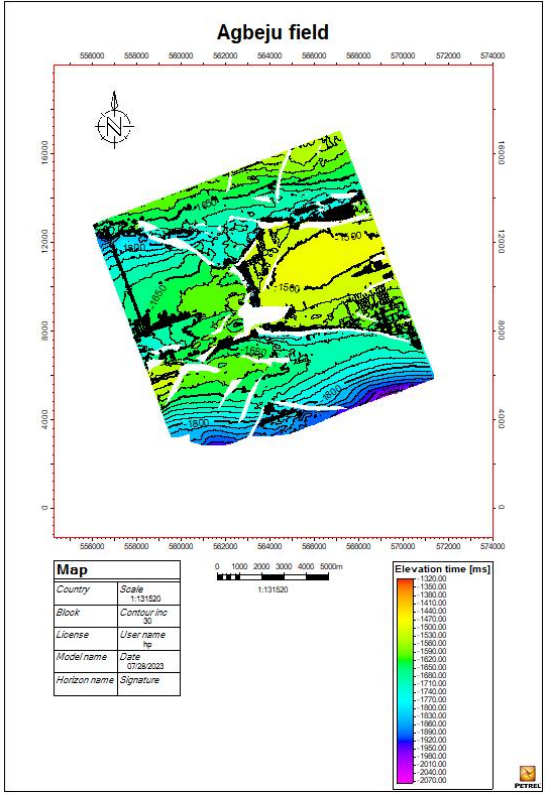


Figure 20: Time structural maps for reservoir sand A at top left (a), reservoir sand B at top right (b) and reservoir sand C at bottom left (c).

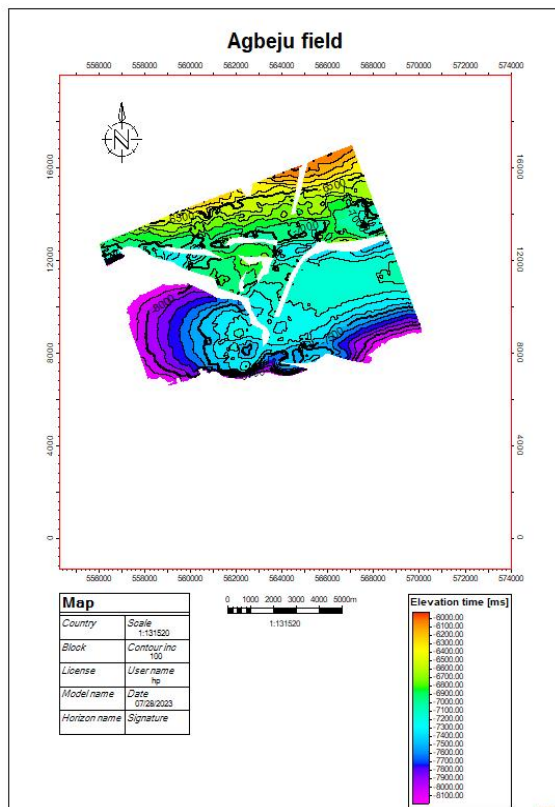
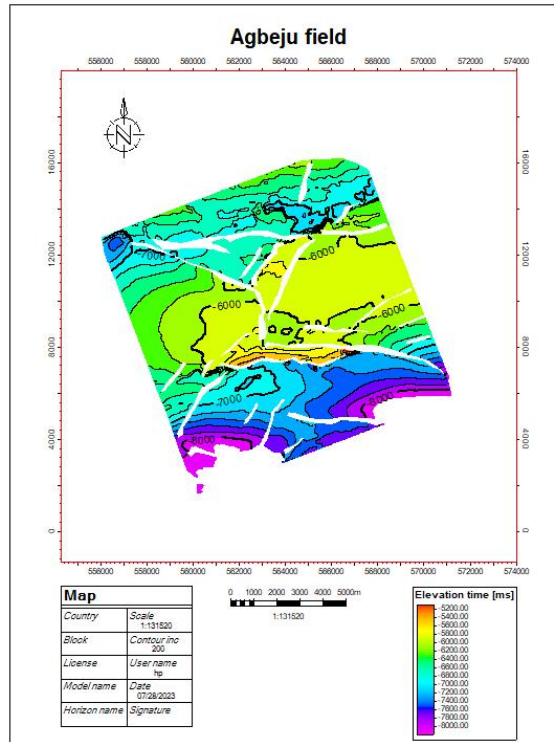
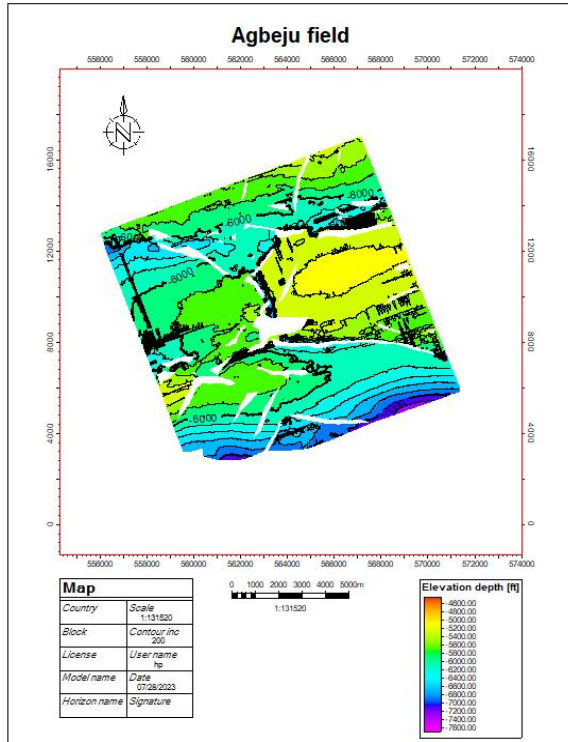


Figure 21: Depth structural maps for reservoir sand A at top left (a), reservoir sand B at top right (b) and reservoir sand C at bottom left (c).

4.2.6 SEISMIC ATTRIBUTE ANALYSIS AND PROSPECT IDENTIFICATION

The time structural maps generated are used for seismic attribute analysis to help identify areas with hydrocarbon presence. Amplitude analysis was done using R.M.S amplitude and Maximum amplitude. This amplitude attributes act as direct hydrocarbon indicators and help identify potential prospect areas.

Prospect identification is the result of the integration of seismic attribute analysis and trap identification where an area with trapping mechanisms in place and hydrocarbon presence defines a prospect. Leads are defined as an area with hydrocarbon presence but lack a defined trapping mechanism within the field.

For sand A, R.M.S amplitude and Maximum amplitude attributes were applied in the figure 22 and figure 23 respectively. Prospect 1 was identified as areas with high amplitude values and a fault assisted closure trapping mechanism.

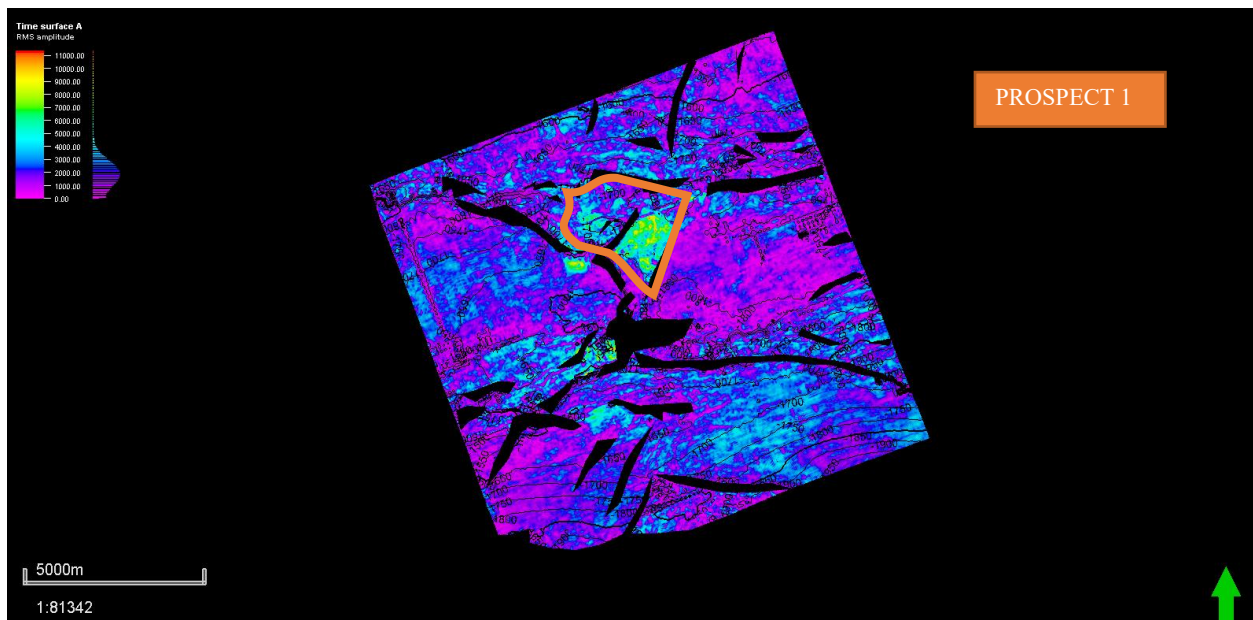


Figure 22: RMS amplitude seismic attribute for sand A top with identified prospects

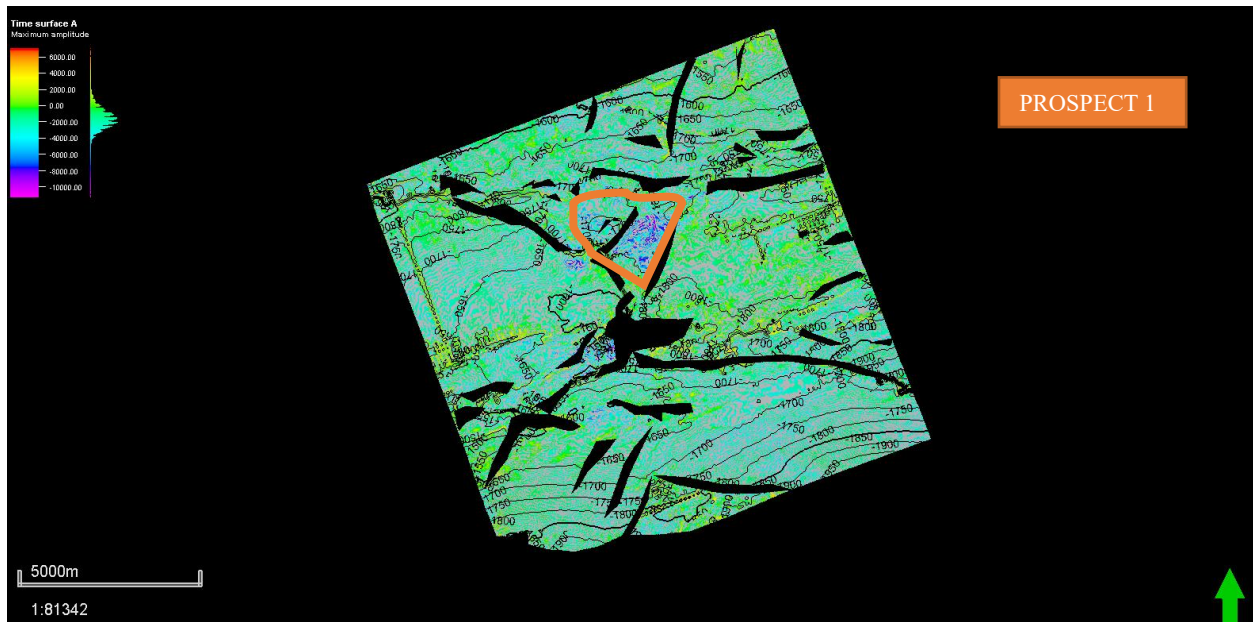


Figure 23: Maximum amplitude seismic attribute for sand A top with identified prospects

For sand B, R.M.S amplitude and Maximum amplitude attributes were applied in the figure 24 and figure 25 respectively. Prospects and leads were identified as areas with high amplitude values. Prospect 1 has a fault assisted closure trap. Prospect 2 has a fault dependent trap. Lead 1, Lead 2 and Lead 3 have fault dependent traps.

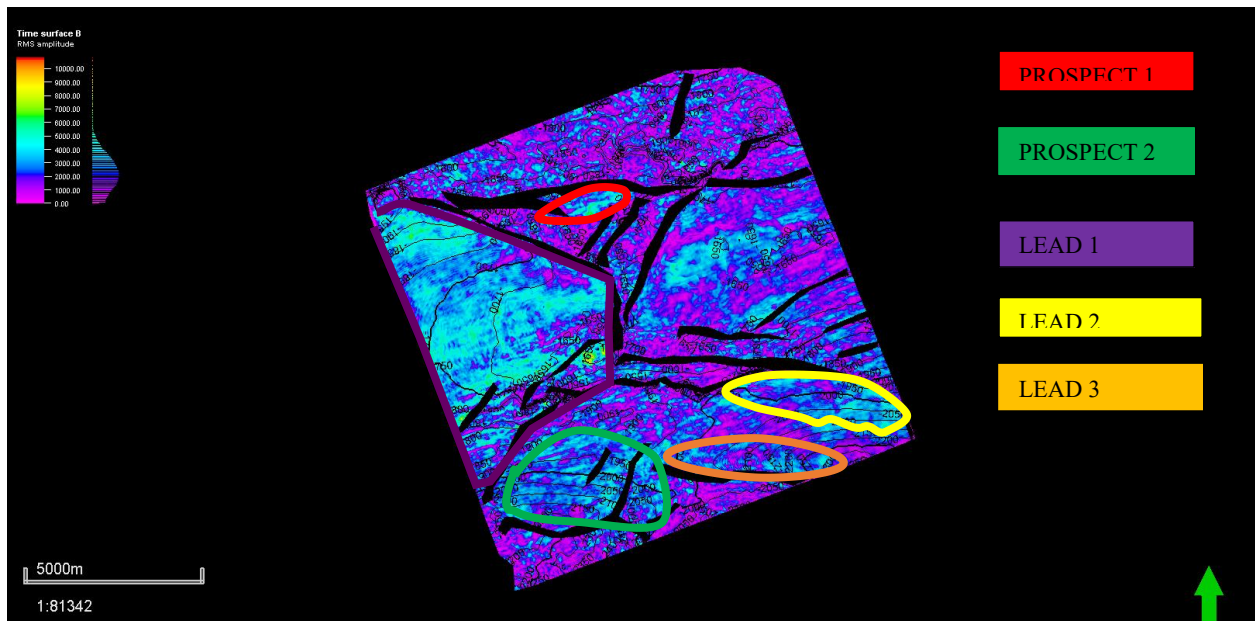


Figure 24: RMS amplitude seismic attribute for sand B top with identified prospects

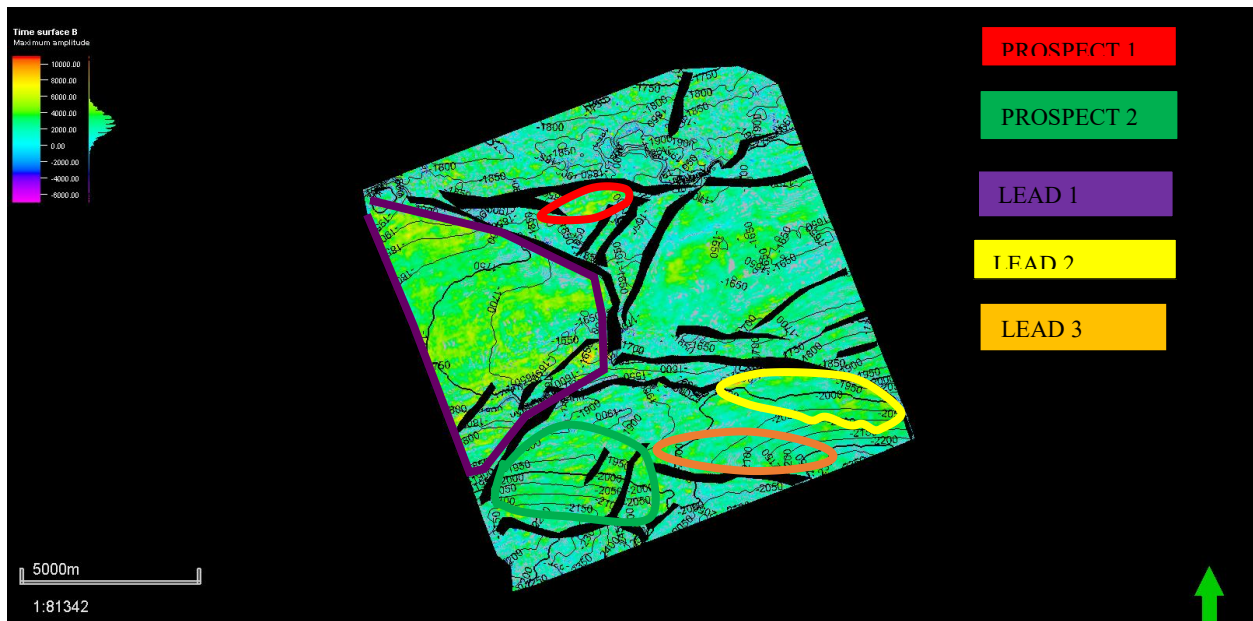


Figure 25: Maximum amplitude seismic attribute for sand B top with identified prospects

For sand C, R.M.S amplitude and Maximum amplitude attributes were applied in the figure 26 and figure 27 respectively. Prospects and leads were identified as areas with high amplitude values. Prospect 1 has a fault assisted closure trap. Lead 1 has a fault dependent trap.

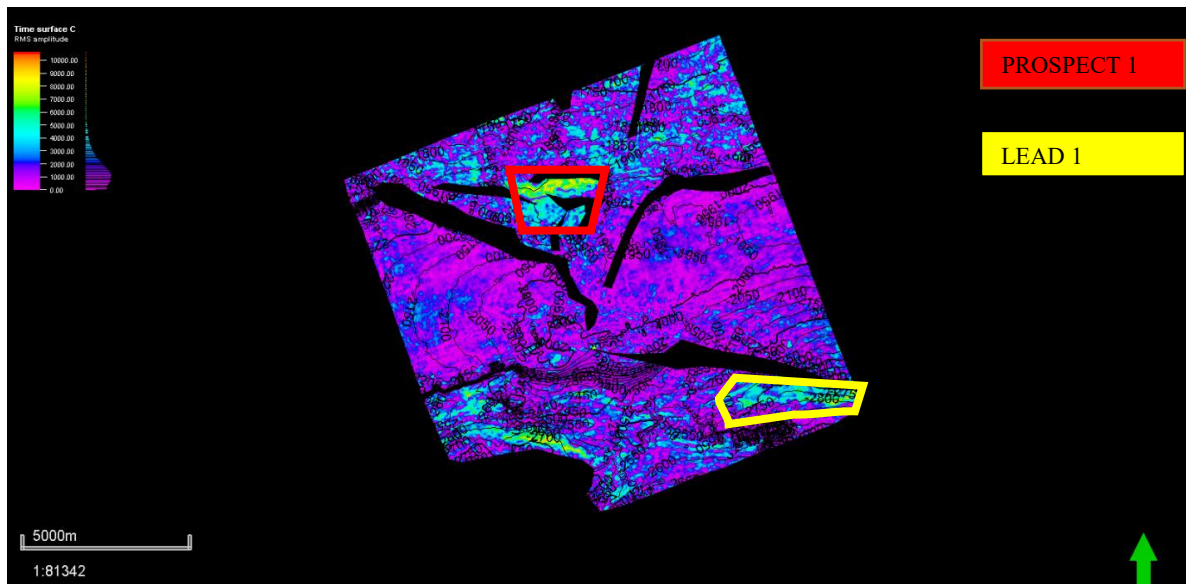


Figure 26: RMS amplitude seismic attribute for sand C top with identified prospects

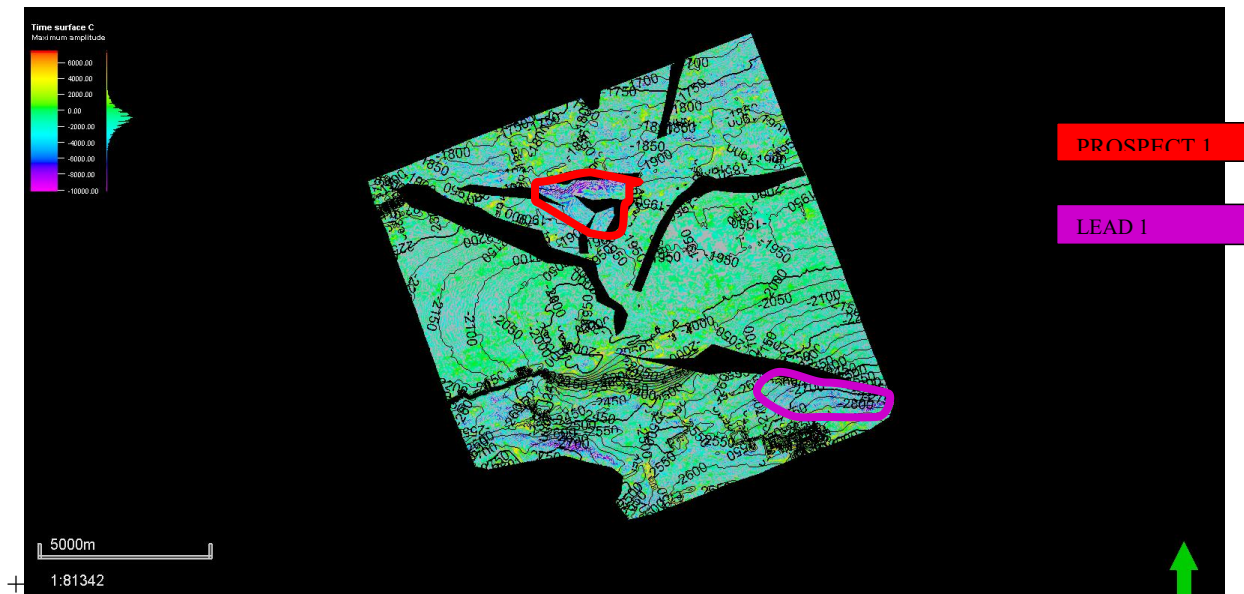


Figure 27: Maximum amplitude seismic attribute for sand C top with identified prospects

4.3 VOLUMETRIC ESTIMATION

Volume estimation is done using the results of petrophysical evaluation and seismic interpretation. The parameters are shown in the table below.

For the petrophysical parameters, the arithmetic mean was used to define the parameters across the five wells while from seismic interpretation; the area was defined from the drilled prospects across the three reservoirs (Sand A, Sand B and Sand C). The drilled prospect corresponds to prospect 1 from all 3 reservoirs from the prospect identification previously in figure 22, figure 24 and figure 26 respectively.

To estimate volume, Gas initially in place (GIIP) was used for Sand A, Sand B and Sand C which have gas bearing intervals while Oil initially in place (OIIP) was used for Sand B and Sand C. The results are shown in the table below.

Table 4: Volumetric estimation of each reservoir

RESERVOIR	AVG Φ_{total}	AVG SW	AVG PAY THICKNESS (Ft)	AREA (acres)	GIIP (SCF)	OIIP (BBL)
SAND A	0.376825	0.5608	64.12	1196.512	554238716	-
SAND B	0.2922	0.726476	114.3933	452.864	162929520	22448823
SAND C	0.28768	0.58988	116.8625	892.186	258195947	83915356

BBL= barrel, SCF= standard cubic feet, MM= million.

CHAPTER FIVE

CONCLUSION AND SUGGESTION FOR FURTHER WORK

5.1 CONCLUSION

This study involves the volumetric estimation of 3 reservoirs (Sand A, Sand B and Sand C) in the drilled prospect in Agbeju field, Niger Delta, using an integrated 3D seismic and well log dataset. The interpretations shows that there are 9 major and 24 minor faults that were mapped, which trend in a predominantly E-W direction and dip southwards, interpreted as syn-depositional deformation as a result of shale gravity tectonics. The 3 reservoirs were identified, delineated and mapped across the seismic data. The average petrophysical properties across the three reservoirs show good to very good values that range between 0.745 - 0.93 net to gross, 0.288 - 0.377 total porosity, and 0.56 - 0.73 water saturation and 64.12ft – 116.8625ft pay thickness.

Seismic attribute analysis shows presence of hydrocarbons identified by strong amplitude contour values on amplitude maps extracted from the time structural maps. Integration of the attribute analysis and trap identification was used to identify various prospects and leads from the three reservoirs.

Integrating the area of the drilled prospects which ranges from 452.864 acres – 1196.512 acres and the result of petrophysical evaluation, volumetric estimation was calculated using GIIP for gas bearing intervals and OIIP for oil bearing intervals. Sand A has an estimated volume of 554MMSCF of gas, Sand B has an estimated volume of 163MMSCF gas and 32.1MMBBL of oil and Sand C has an estimated volume of 258MMSCF of gas and 83.9MMBBL of oil. The reservoirs can be ranked from Sand A, Sand C to Sand B based on the hydrocarbon volume estimates.

5.2 SUGGESTION FOR FURTHER WORK

New wells should be drilled to appraise the prospective areas and help delineate fluid contacts. Seismic data should be acquired to understand and characterize lead areas.

REFERENCES

Anderson, E. M., (1942). The Dynamics of Faulting and Dyke Formation with Applications to Britain. Edinburgh.

- Anene, N. O., Ehinola, O. A., & Eyinla, D. S. (2018).** Sub-surface mapping and reservoir evaluation of “Enena” field, offshore Niger Delta. *J Appl Geol Geophys*, 6, 65-73.
- Archie G. E., (1942).** The electrical resistivity log as an aid in determining some reservoir characteristics. *Trans Am Inst Mech Eng* 146: 54-62.
- Asadu, A. N., Omor-irabor, O. O., & Ibe, K. A., (2015).** Source Rock Characterization of Agbada Formation in Well Z, Offshore Niger Delta. *International Journal for Research in Emerging Science and Technology*.
- Asquith, G. & Krygowski, D. (2004).** *Basic Well Log Analysis*, 2nd ed., Tulsa, Oklahoma: American Association of Petroleum Geologists, 1-2, 31-32.
- Beka, F. T., and Oti, M. N., (1995).** The distal offshore Niger Delta: frontier prospects of a mature petroleum province, in, Oti, M.N., and Postma, G.. eds., *Geology of Deltas*: Rotterdam, A.A. Balkema, pp. 237-241.
- Bustin, R. M. (1988).** Sedimentology and characteristics of dispersed organic matter in Tertiary Niger Delta: origin of source rocks in a deltaic environment. *American Association of Petroleum Geologists Bulletin*, 72, pp. 277-298.
- Bowen, B. E.; Hall, D. J.; Rosen, R. N., and Shaffor, B. L., (1994).** Sequence stratigraphic and structural framework of southeast Niger Delta shelf. *NAPE Bulletin*, Vol. 9(1), pp. 51-58.
- Dim, C. and Onuoha, K. (2017).** Insight into Sequence Stratigraphic and Structural Framework of the Onshore Niger Delta Basin: Integrating Well Logs, Biostratigraphy, and 3D Seismic Data. *Arabian Journal of Geosciences*, 10, Article No. 300
- Doust, H. and Omatsola, E. (1990).** Niger Delta, in, Edwards, J.D. and Santogrossi, P.A. eds., *Divergent/passive Margin Basins*, AAPG Memoir 48: Tulsa, American Association of Petroleum Geologists, pp. 239-248.
- Edwards, J. D., and Santogrossi, P. A., (1990).** Summary and Conclusions, in, Edwards, J.D. and Santogrossi, P.A. ed., *Divergent/passive Margin Basins*, AAPG Memoir48: Tulsa, American Association of Petroleum Geologists, pp. 239-248.
- Ejedawe, J. E., (1981).** Patterns of incidence of oil reserves in Niger Delta Basin. *American Association of Petroleum Geologists*, 65. pp. 1574-1585

- Ekweozor C. M., Okogun J. I., Ekong D. E. U. and Maxwell J. R., (1979).** Preliminary organic geochemical studies of samples from the Niger Delta, Nigeria: Part 1, Analysis of crude oils for triterpanes: *Chemical Geology*; 27: 11-28.
- Ekweozor, C. M. and Okoye, N. V., (1980).** Petroleum source-bed evaluation of Tertiary Niger Delta. *American Association of Petroleum Geologists Bulletin*, 64, pp. 1251-1259.
- Ekweozor, C. M. and Daukoru, E. M., (1984).** Petroleum source bed evaluation of Tertiary Niger Delta-reply: *American Association of Petroleum Geologists Bulletin*, 68, pp. 390-394.
- El-Mowafy, H. and Marfurt , K., (2008).** Structural Interpretation of the Middle Frio Formation using 3D Seismic and Well logs: An Example from the Gulf Coast of the United States. *The Leading Edge*, vol. 27, No 7, p 840 – 848.
- Emujakporue, G., Ekine, A., & Nwosu, L. (2019).** Evaluation of Time-Temperature Index and Vitrinite Reflectance for Hydrocarbon Maturity in Parts of Niger Delta Sedimentary Basin, Nigeria. *International Journal of Research and Innovation in Applied Science*, 4(11), 7-15.
- Evamy, B. D., Haremboure, J., Kamerling, P., Knaap, W. A., Molloy, F. A. and Rowlands, P. H., (1978).** Hydrocarbon habitat of tertiary Niger Delta: *American Association of Petroleum Geologists Bulletin*, 62, pp. 277-298.
- Frost, B. R., (1977).** A Cretaceous Niger Delta Petroleum System, in, *Extended Abstracts, AAPG/ABGP Hedberg Research Symposium, Petroleum Systems of the South Atlantic Margin*, November 16-19, 1997, Rio de Janeiro, Brazil
- Haack, R. C., Sundararaman, P. and Dahl, J., (1997).** Niger Delta petroleum System, in, *Extended Abstracts, AAPG/ABGP Hedberg Research Symposium, Petroleum Systems of the South Atlantic Margin*, November 16-19, 1997. Rio de Janeiro, Brazil.
- Hunt, J. M., (1990).** Generation and migration of petroleum from abnormally pressured fluid compartments: *American Association of Petroleum Geologists Bulletin*, v. 74, pp. 1-12.
- Illo, C. A., Ugbor, C. C., Eradiri, J. N., & Emedo, C. O. (2022).** Prospect identification and reservoir characterization using seismic and petrophysical data in ‘Famito’ field, onshore Niger Delta, Nigeria. *Arabian Journal of Geosciences*, 15(4), 348.

- Jahn, F., Cook, M., Graham, M. (2008).** Hydrocarbon Exploration and Production. Germany: Elsevier Science. 27 -42, 146-147.
- Kulke, H., (1995).** Nigeria, in: Kulke, H., ed., Regional Petroleum Geology of the World. Par II Africa, America, Australia and Antarctica: Berlin, Gebrüder Borntraeger, pp. 143-172.
- Lambert-Aikhionbare, D. O. and Ibe, A.C., (1984).** Petroleum source-bed evaluation of the Tertiary Niger Delta: discussion. American Association of Petroleum Geologists Bulletin, 68, pp. 387-394.
- Lehner, P. and De Ruiter, P. A. C., (1977).** Structural history of Atlantic margin of Africa. American Association of Petroleum Geologists Bulletin, 61: 961- 981.
- Leiphart, D. J., & Hart, B. S. (2001).** Case history: Comparison of linear regression and a probabilistic neural network to predict porosity from 3-D seismic attributes in Lower Brushy Canyon channeled sandstones, southeast New Mexico. *Geophysics*, 66(5), 1349-1358.
- North, F. I., (1985).** Petroleum Geology. Springer, Berlin.
- Nton, M. E., & Adeyemi, M. O. (2021).** Evaluation of Hydrocarbon Reserve in AD Field, Offshore Niger Delta. *Open Journal of Geology*, 11(5), 155-174.
- Nwachukwu, J. I., and Chukwurah, P. I., (1986).** Organic matter of Agbada Formation, Niger Delta, Nigeria: American Association of Petroleum Geologists Bulletin, v. 70, p. 48-55.
- Nwozor, K. K., Omudu, M. L., Ozumba, B. M., Egbuachor, C. J., Onwuemesi, A. G., & Anike, O. L. (2013).** Quantitative evidence of secondary mechanisms of overpressure generation: Insights from parts of Onshore Niger Delta, Nigeria. *Petroleum technology development journal*, 3(1), 64-83.
- Obiora D. N., Gbenga D. and Ogobiri G., (2016).** Reservoir Characterization and Formation Evaluation of a “Royal Onshore Field”, Southern Niger Delta using Geophysical Well Log Data. *Journal Geological Society of India*; 87: 591-600.
- Ogbamikhumi A. and Aderibigbe O. T., (2019).** Velocity modelling and depth conversion uncertainty analysis of onshore reservoirs in the Niger Delta basin. *Journal of the Cameroon Academy of Sciences*, 14(3), 239-247

- Okwoli E., Obiora D. N., Adewoye O., Chukudebelu J. U., and Ezema P. O., (2015).** Reservoir characterization and volumetric analysis of “LONA” Field, Niger Delta, using 3-D seismic and well log data. *PetCoal*; 57(2): 108-119.
- Okpogo, E. U., Abbey, C. P., & Atueyi, I. O., (2018).** Reservoir characterization and volumetric estimation of Orok Field, Niger Delta hydrocarbon province. *Egyptian journal of petroleum*, 27(4), 1087-1094.
- Omoja, U. C., & Obiekezie, T. N. (2021).** Evaluation of Petrophysical Parameters of Reservoir Sand Wells in Uzot-Field, Onshore Niger Delta Basin, Nigeria. *Journal of Applied Sciences and Environmental Management*, 25(2), 157-171.
- Osinowo, O. O., Ayorinde, J. O., Nwankwo, C. P., Ekeng, O. M., & Taiwo, O. B., (2018).** Reservoir description and characterization of Eni field Offshore Niger Delta, southern Nigeria. *Journal of Petroleum Exploration and Production Technology*, 8(2), 381-397
- Owolabi, O. O., Longjohn, T. F. & Ajienska J. A., (1994).** An empirical Expression for Permeability in Unconsolidated Sands of Eastern Niger Delta: *Journal of Petroleum Geology* 17 (1), 111-116.
- Reijers, T. J. A., Petters, S. W., and Nwajide, C. S., (1997).** The Niger Delta Basin, in Selley, R.C., ed., *African Basins--Sedimentary Basin of the World 3: Amsterdam, Elsevier Science*, pp. 151-172
- Rider, M. H., (2002).** *The Geological Interpretation of Well Logs: Whittles Publishing, 2nd Edition. Aberdeen, UK. 226-260.*
- Sagan, J. A., & Hart, B. S. (2006).** Three-dimensional seismic-based definition of fault-related porosity development: Trenton–Black River interval, Saybrook, Ohio. *AAPG bulletin*, 90(11), 1763-1785.
- Schlumberger, (1974).** *Log Interpretation Chart, Schlumberger Educational Services, New York.*
- Shannon, P. M., and Naylor N., (1989).** *Petroleum Basin Studies: London, Graham and Trotman Limited, pp 153-169.*
- Shepherd, M., (2009).** Rock and Fluid Properties. *Oil field production geology. AAPG Memoir*, 91: 65- 68.

- Short, K. C. and Stauble, J., (1967).** Outline geology of the Niger Delta. AAPG Bull 5, pp. 761-779.
- Sonibare O., Alimi H., Jarvie D., Ehinola O. A., (2008).** Origin and occurrence of crude oil in the Niger Delta, Nigeria. Journal of Petroleum Science and Engineering; 61(2-4):99-107.
- Stacher, P., (1995).** Present understanding of the Niger Delta hydrocarbon habitat, in, Oti, M.N., and Postma, G., eds., Geology of Deltas: Rotterdam, A.A. Balkema, p. 257-267.
- Stacy, C. A., Nathaniel, H. B. and Luke, E. H., (2010).** Reservoir characterization and facies prediction within the Late Cretaceous Doe Creek Member, Valhalla field, west-central Alberta, Canada. AAPG Bulletin, 94(1): 1-25.
- Tuttle M. L. W., Charpentier R. R., and Brownfield M. E., (1999).** The Niger Delta Petroleum System: Niger Delta Province, Nigeria Cameroon, and Equatorial Guinea, Africa. Open-File Report 99-50-H
- Varhaug, M., (2016).** Basic Well Log Interpretation: Oilfield Review
- Weber, K. J., (1987).** Hydrocarbon distribution patterns in Nigerian growth fault structures controlled by structural style and stratigraphy. Journal of Petroleum Science and Engineering, 1, pp. 91-104.
- Weber, K. J. and Daukoru, E. M., (1975).** Petroleum Geology of the Niger Delta: Proceedings of the Ninth World Petroleum Congress, volume 2, Geology: London, Applied Science Publishers, Ltd., pp. 210-221
- Whiteman, A., (1982).** Nigeria: Its Petroleum Geology, Resources and Potential: London, Graham and Trotman, pp. 394.
- Wobo, C., & Ideozu, R. (2022).** Petrophysical Properties and Reservoir Modeling of Kala Field, Eastern Niger Delta, Nigeria.
- Wyllie, M. R. J., Gregory, A. R., & Gardner, G. H. F., (1958).** An experimental investigation of factors affecting elastic wave velocities in porous media. Geophysics, 23(3), 459-493.